Chapter 3

Recent Change in the Arctic and the Arctic Oscillation

3.1. The Arctic Oscillation

During the 1990s, a quiet revolution took place in the perception of the Arctic (Carmack *et al.*, 1997; Dickson, 1999; Johannessen *et al.*, 1995; Johnson and Polyakov, 2001; Kerr, 1999; Levi, 2000; Macdonald, 1996; Macdonald *et al.*, 1999a; Maslanik *et al.*, 1996; Maslowski *et al.*, 2000; McPhee *et al.*, 1998; Morison *et al.*, 1998, 2000; Parkinson *et al.*, 1999; Polyakov and Johnson, 2000; Quadfasel *et al.*, 1991; Smith, 1998; Steele and Boyd, 1998; Vanegas and Mysak, 2000; Vörösmarty *et al.*, 2001; Walsh, 1991; Welch, 1998; Weller and Lange, 1999). Despite early evidence of cyclical change in northern biological populations and ice conditions (e.g., Bockstoce, 1986; Gudkovich, 1961; Vibe, 1967), the general view among many western physical scientists throughout the 1960s to 1980s was that the Arctic was a relatively stable place (Macdonald, 1996). This view has been replaced by one of an Arctic where major shifts can occur in a very short time, forced primarily by natural variation in the atmospheric pressure field associated with the Northern-hemisphere Annual Mode.

The Northern-hemisphere Annual Mode, popularly referred to as the Arctic Oscillation (AO) (Wallace and Thompson, 2002), is a robust pattern in the surface manifestation of the strength of the polar vortex (for a very readable description, see Hodges, 2000). The AO correlates strongly (85-95%) with the more commonly used indicator of large-scale wind forcing, the North Atlantic Oscillation (NAO) (the NAO is the normalized gradient in sea-level air pressure between Iceland and the Azores – see for example, Deser, 2000; Dickson *et al.*, 2000; Hurrell, 1995; Serreze *et al.*, 2000). In this report the AO and NAO are used more or less interchangeably because they carry much the same information. It is recognized, however, that in both cases the term 'oscillation' is rather misleading because neither index exhibits quasi-periodic behaviour (Wallace and Thompson, 2002). The AO captures more of the hemispheric variability than does the NAO which is important because many of the recent changes associated with the AO have occurred in the Laptev, East Siberian, Chukchi and Beaufort Seas – a long way from the NAO's center of action (Thompson and Wallace, 1998). Furthermore, the Bering Sea and the Mackenzie Basin are both influenced to some degree by atmospheric processes in the North Pacific (e.g., the Pacific Decadal Oscillation; see also Bjornsson *et al.*, 1995; Niebauer and Day, 1989; Stabeno and Overland, 2001), whereas the Baffin Bay ice climate appears to have an association with the Southern Oscillation (Newell, 1996), and the Canadian Arctic Archipelago and Hudson Bay probably respond to various atmospheric forcings as yet not fully understood.

Although the AO is an important component of change in Arctic climate, it accounts for only 20% of the variance in the atmospheric pressure field and many other factors can determine the atmospheric forcing. Because the AO is usually 'smoothed', it does not adequately represent events and short-term variations which are known to be important for the delivery of contaminants to the Arctic and possibly also locally important in forcing ice and surface water motion (see for example, Sherrell *et al.*, 2000; Welch *et al.*, 1991). It is important to note that one of the projections of climate change is that cyclonic activity will increase; extreme events may therefore become a prominent component of atmospheric transport in the coming century. The earliest significant rain event on record (May 26, 1994), which was observed widely throughout the Canadian Arctic Archipelago may have represented an example of this (see also Graham and Diaz, 2001; Lambert, 1995).

Around 1988 to 1989, the AO entered a positive phase of unprecedented strength (Figures 3·1 a and c, next page). The sea-level pressure (SLP) distribution pattern of the AO for winter and summer (Figures 3·1 b and d) shows that this positive shift in AO is characterized by lower than average SLP distributed somewhat symmetrically over the pole (the blue-isoline region on Figures 3·1 b and d) and higher SLP over the North Atlantic and North Pacific in winter and over Siberia and Europe in summer. As might be expected from examination of the AO SLP pattern (Figures 3·1 b and d), when the AO index is strongly positive conditions become more 'cyclonic' – i.e., atmospheric circulation becomes more strongly counterclockwise (Proshutinsky and Johnson, 1997; Serreze *et al.*, 2000).

In discussing change it is important to distinguish between variability, which can occur at a variety of time scales (Fischer *et al.*, 1998; Polyakov and Johnson, 2000) and trends caused, for example, by GHG warming. It has been suggested that locking the AO into a positive mode might actually be one way that a trend forced by GHGs can manifest itself in the Arctic (Shindell *et al.*, 1999). Others, however, consider that the extraordinary conditions of the 1990s were produced naturally by a reinforcing of short (5-7 yr) and long (50-80 yr) time-scale components of SLP variation (Polyakov and Johnson, 2000; Wang and Ikeda, 2001), and that GHG forcing will affect the mean property fields rather than alter the AO itself (Fyfe, 2003; Fyfe *et al.*, 1999). Longer records of the NAO index (Figure 3·16 a, page 18) indeed suggest that there have been other periods of high AO index during the past 150 years (e.g., 1900-1914), but none as strong as that experienced during the early 1990s. Recent data suggest that the AO index has decreased and that the Arctic system has to some degree begun to return to 'normal conditions' (Björk *et al.*, 2002; Boyd *et al.*, 2002; Johnson *et al.*, 1999).

The contrast in conditions between the Arctic in the 1960s, 1970s and 1980s (with a generally low/negative AO index) and the Arctic in the early 1990s (with an exceptionally high/positive AO index) provides an extraordinary opportunity to investigate how the Arctic might respond to climate change. Similarity between climate-

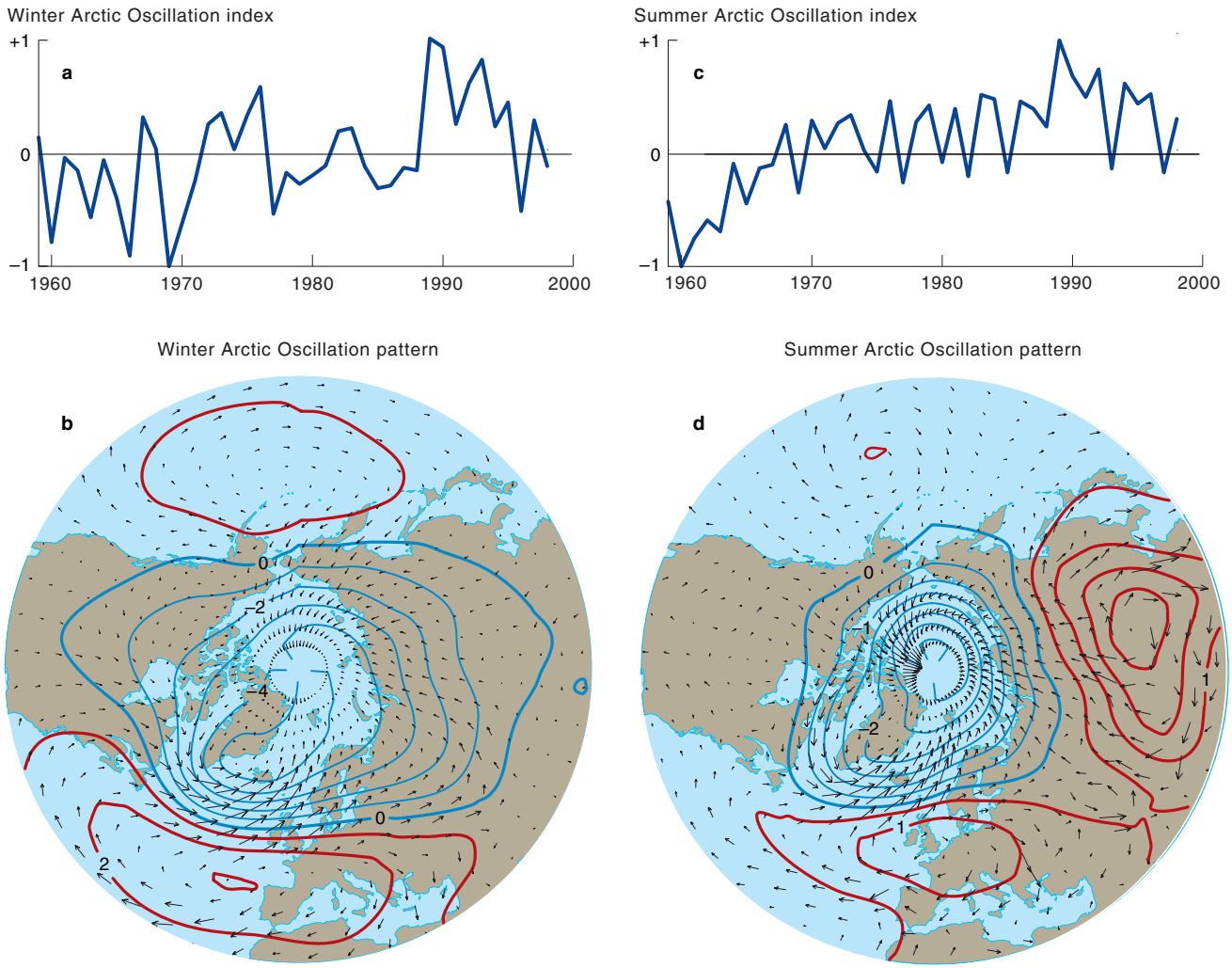

Figure 3·1. The Arctic Oscillation. The figure illustrates a) variability in the AO index between 1958 and 1998 in winter; b) the associated winter sea-level pressure pattern; c) variability in the AO index between 1958 and 1998 in summer; and d) the associated summer sea-level pressure pattern. To recreate atmospheric pressure patterns during the period in question, the winter (b) and summer (d) AO patterns would be multiplied by their respective indices (a, c) and added to the mean pressure field. Thus the high winter AO index in the early 1990s implies anomalously low pressure over the pole in the pattern shown in (b). Small arrows show the geostrophic wind field associated with the AO pattern with longer arrows implying stronger winds.

change projections and AO-induced change suggests that examining the differences between AO^- and AO^+ states should provide insight into the likely effects of climate change forced by GHG emissions. Variation in SLP, as reflected by the AO index, demonstrates that the Arctic exhibits at least two modes of behaviour (Morison *et al.*, 2000; Proshutinsky and Johnson, 1997) and that these modes cascade from SLP into wind fields, ice drift patterns, watermass distributions, ice cover and probably many other environmental parameters.

The Arctic is to a large degree constrained by overarching structures and processes in how it can respond to change. As illustrated in previous assessments, the Arctic Ocean is, and will remain, a 'mediterranean' sea, much influenced by land–ocean interaction and with restricted exchange with other oceans (Figure 1·1). Topography, bathymetry and global distribution of salinity in the ocean, require that water from the Pacific Ocean will predominantly flow *in* to the Arctic and the shallow sill at Bering Strait (50 m) guarantees that only surface water will be involved in this exchange. Pacific water will remain above Atlantic Layer water which is denser. Deep-basin water communicates predominantly with the Atlantic Ocean through the deep connection at Fram Strait. Ocean circulation within the Arctic is tightly tied to bathymetry through topographic steering of currents (Rudels *et al.*, 1994). Considering these kinds of constraints, rapid change can occur in ocean-current pathways or in the source or properties of the water carried by currents when, for example, fronts shift from one bathymetric feature to another (McLaughlin *et al.*, 1996; Morison *et al.*, 2000), when a given current strengthens or weakens (Dickson *et al.*, 2000), when source-water composition alters (Smith *et al.*, 1998; Swift *et al.*, 1997), or when relative strength of outflow varies between the Canadian Arctic Archipelago and Fram Strait (Macdonald, 1996), but not by reversal of flow in boundary currents or reversal of mean flow in the Bering Strait or out through the Archipelago.

Change associated with the Northern-hemisphere Annual Mode requires that consideration be given to large-scale variability in the Arctic; the fact that physical pathways can change rapidly needs to be recognized in greater detail, and the potential effects of GHG emissions against this naturally variable background should be assessed.

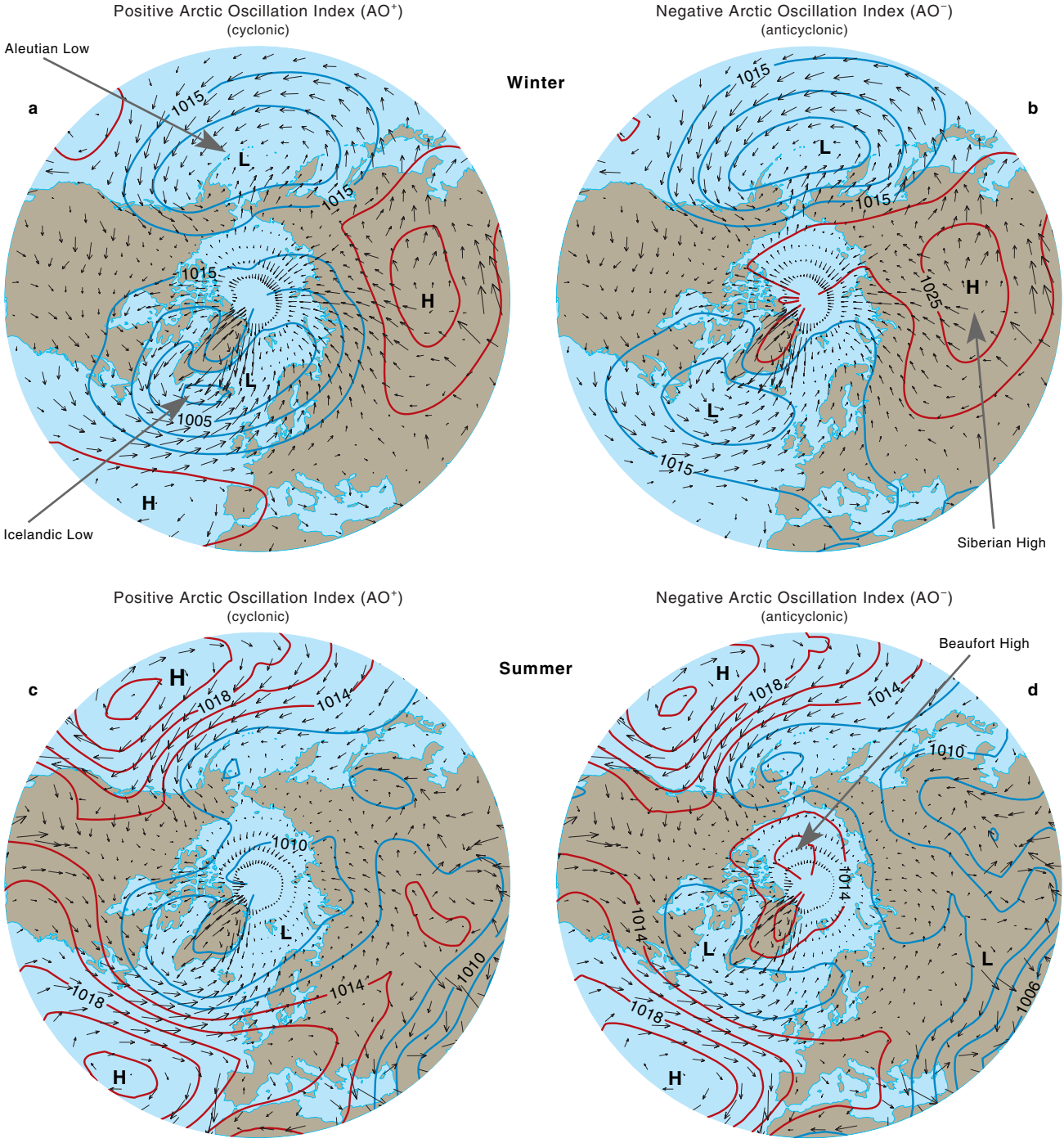

Figure 3·2. Atmospheric pressure fields and wind stream lines in the Northern Hemisphere. The figure illustrates a) strong AO+ conditions in winter; b) strong AO− conditions in winter; c) strong AO+ conditions in summer; and d) strong AO− conditions in summer.

3.2. Winds

Winds transport contaminants directly to the Arctic by delivering volatile and semi-volatile chemicals, and chemicals attached to fine particulates, from the south in timescales as short as a few days (Bailey *et al.*, 2000; Barrie *et al.*, 1998; Halsall *et al.*, 1998; Hung *et al.*, 2001; Stern *et al.*, 1997). Over the longer term, spanning months to years, winds deliver volatile and semi-volatile contaminants through a series of hops, as airborne chemicals become deposited onto surfaces (water, soil or vegetation) and then re-volatilized during, for example, summer warming. Winds also provide the primary forcing for ice drift and surface ocean currents (Mysak, 2001; Proshutinsky and Johnson, 1997) thereby indirectly affecting transport by these two media as well.

To understand how swings in the AO can affect atmospheric circulation, AO+ and AO− wind field/SLP maps have been constructed for winter (Figures 3·2 a and b) and summer (Figures 3·2 c and d) by adding (AO+) or subtracting (AO−) the patterns in Figures 3·1 b and d to/from the mean pattern for the period of record in the time series (1958-1998). The changes discussed in the following paragraphs can be considered generally as representing the difference between conditions during the 1960s to 1970s (low/negative AO index) and during the early 1990s (high/positive AO index) (see for example, Proshutinsky and Johnson, 1997).

In winter (Figures 3·2 a and b), the lower tropospheric circulation is dominated by high pressure over the continents and low pressure over the northern Pacific Ocean (Aleutian Low) and Atlantic Ocean (Icelandic Low). The Siberian High tends to force air on its western side into the Arctic, acting as an effective atmospheric conduit from industrialized regions of Siberia and Eastern Europe to the High Arctic. The high-pressure ridge over North America then forces air southward giving a net transport out of Eurasia into the Arctic, across the Arctic and south over North America. The Icelandic Low produces westerly winds over the eastern North Atlantic and southerly winds over the Norwegian Sea providing a second conduit by which airborne contaminants from eastern North America and Europe can rapidly reach the Arctic. Finally, the Aleutian Low tends to steer air that has crossed the Pacific from Asia up into Alaska, the Yukon, and the Bering Sea (Bailey *et al.*, 2000; Li *et al.*, 2002; Wilkening *et al.*, 2000). During winter, these three routes into the Arctic – southerlies in the Norwegian Sea (40%), over Eastern Europe/Siberia (15%), and over the Bering Sea (25%) account for about 80% of the annual south-to-north air transport (Iversen, 1996).

With a higher AO index (Figure 3·2 a), the Icelandic Low intensifies and extends farther into the Arctic across the Barents Sea and into the Kara and Laptev Seas (Johnson *et al.*, 1999). This has the effect of increasing the wind transport east across the North Atlantic, across southern Europe and up into the Norwegian Sea. During high NAO winters, westerlies onto Europe may be as much as 8 m/s (~700 km/day) stronger (Hurrell, 1995). At the same time, strong northerly winds are to be found over the Labrador Sea (Mysak, 2001).

The extension of the Icelandic Low into the Arctic also implies an effect of the AO on storm tracks. During the strong AO^+ conditions of the early 1990s, there was a remarkable increase in the incidence of deep storms, to around 15 per winter, and these storms penetrated farther into the Arctic (Dickson *et al.*, 2000; Maslanik *et al.*, 1996; Semiletov *et al.*, 2000). Increased cyclone activity increases poleward transport of heat and other properties carried by the air masses involved. Anomalous southerly airflow over the Nordic Seas enhances the connection between industrial regions of North America and Europe and the Arctic. At the same time, increased cyclones enhance transfer of contaminants from the atmosphere to the surface as a consequence of increased precipitation. Deep within the Arctic, the high SLP ridge that extends across Canada Basin during AO^- conditions (the Beaufort High), disappears and withdraws toward Russia (Johnson *et al.*, 1999; Morison *et al.*, 2000). It is worth noting that the Pacific mean atmospheric pressure field and wind patterns appear to change little between strong positive and strong negative phases of the AO in winter. Penetration of air from the Pacific into the Arctic is hindered by the mountain barrier along the west coast of North America where intensive precipitation also provides a mechanism to transfer contaminants and aerosols to the surface (Figures 3·2 a and b).

Summer pressure fields and air-flow patterns are markedly different from those of winter (compare Figures 3·2 a, b, c, and d). In summer, the continental high-pressure cells disappear and the oceanic low-pressure cells weaken with the result that northward transport from low latitudes weakens (Figures 3·2 c and d). According to Iversen (1996) summer accounts for only 20% of the annual south-to-north air transport (southerlies in the Norwegian Sea (10%), Eastern Europe/Siberia (5%), and Bering Sea (5%)). The streamlines show that winds provide a means to transport contaminants from industrialized North America and Europe to the North Atlantic but penetration into the Arctic weakens. In the North Pacific, there remain atmospheric pathways to move air masses into the Gulf of Alaska from the east coast of Asia (Figures 3·2 c and d). During AO^+ conditions in particular, the Beaufort High weakens or disappears (Figures 3·2 a and c), altering mean wind fields.

3.3. Surface air temperature

A strong trend of warming has been observed in the Arctic for the period from 1961 to 1990 (Figure 3·3 a). This warming, which has been especially evident over northwestern North America and Siberia, has been accompanied by cooling in northeastern Canada, Baffin Bay, and West Greenland. An almost identical pattern of warming to that shown in Figure 3·3 a is produced by taking the difference between mean surface air temperatures during periods of AO^+ and AO^- conditions (Wallace and Thompson, 2002). Due to an extensive temperature record collected from drifting buoys, manned drifting stations, and land stations, direct relationships can be drawn between air surface temperature over sea and land in the Arctic and the changes in pressure field discussed in section 3.2. Over the period 1979 to 1997, a trend of +1°C per decade was found for winter surface air temperature (SAT) in the eastern Arctic Ocean, offset by a trend of –1°C per decade in the western Arctic Ocean (Rigor *et al.*, 2000). However, in spring almost the entire Arctic Ocean shows significant warming – as much as 2°C per decade in the eastern Arctic where a trend toward lengthened melt season was also observed. The trend in increasing SAT over the ocean is matched by temperature increases over Arctic land masses of 2°C per decade during winter and spring and annual increases of perhaps 0.8°C per decade (Figure 3·3 a). Records of annual temperature anomalies since 1900 (Figure 3·3 b) clearly show the warming trend since the 1970s, but note also that a similar episode of warming occurred in the 1930s to 1940s. Taken together, the trends in SAT over the central Arctic Ocean suggest that warming has occurred predominantly during January to July (Figure 3·3 c). Over half of the change in SAT in Alaska, Eurasia and the eastern Arctic Ocean has been ascribed to the AO, but less than half in the western Arctic (see Dickson *et al.*, 2000; Rigor *et al.*, 2000; Serreze *et al.*, 2000). The temperature changes associated with the AO are considered large enough to have an immediate effect on polar circulation (Morison *et al.*, 2000).

3.4. Precipitation and runoff

Precipitation is a key pathway for contaminant transport (Figure 1·2); rain, snow and fog scavenge aerosols and gasses from the atmosphere to deposit them at the surface (Chernyak *et al.*, 1996; Li *et al.*, 2002; Macdonald *et al.*, 2000a; Mackay and Wania, 1995; Malcolm and Keeler, 2002; Wania and Mackay, 1999). Scavenging by precipitation may be relatively weak in the desert-like

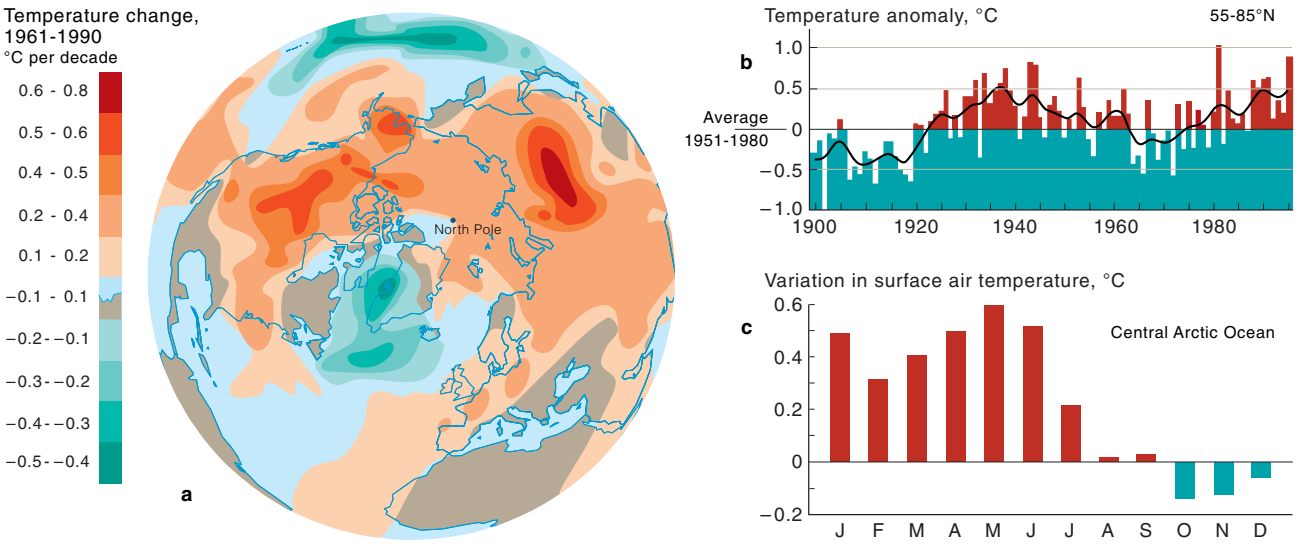

Figure 3·3. Temperature trends for the Arctic. This figure illustrates a) surface temperature trends over the Northern Hemisphere between 1961 and 1990 (courtesy of the Climate Monitoring and Data Interpretation Division of the Atmospheric Environment Service of Canada; Stewart *et al.*, 1998); b) annual temperature anomalies (55-85°N) for the period 1900 to 1995 set against the average for 1951 to 1980, showing that the high temperatures of the late 1980s and 1990s are matched by equally high temperatures during the 1930s and 1940s (adapted from Serreze *et al.*, 2000); and c) the average monthly variation in surface air temperature of the central Arctic Ocean between 1979 and 1995 showing that recent warming is mainly a winter–spring phenomenon (adapted from Serreze *et al.*, 2000).

conditions that prevail over much of the High Arctic. For example, mean precipitation for the Arctic Ocean is estimated to be about 25.2 cm/yr and evaporation about 13.6 cm/yr, yielding a net moisture flux to ground of 11.9 cm/yr (Barry and Serreze, 2000). The precipitation over land in the Arctic drainage basins is somewhat greater as implied by runoff yield (precipitation minus evaporation (P−E)) estimates of 21.2 cm/yr from the network of gauged discharge by rivers (Lammers *et al.*, 2001).

Given the changes in winds (Figure 3·2) and temperature that occur with shifts in the AO, it is to be expected that precipitation and evaporation within the Arctic will also be affected, both in amount and seasonality (Serreze *et al.*, 2000). Due to sparse monitoring networks and short time-series, it is difficult to assess with confidence the spatial or temporal variation of precipitation within the Arctic. Nevertheless, records suggest that precipitation has increased over northern Canada by about 20% during the past 40 years (Serreze *et al.*, 2000). The increase in southerly winds in the Norwegian Sea in winter and the penetration of cyclones from the Atlantic into the Barents, Kara and Laptev Seas, when the AO (or NAO) index is high, is reflected in increased moisture flux and precipitation during autumn and winter, especially in the area between 10°W and 50°E (Figure 3·4 a; Dickson *et al.*, 2000; Ser-

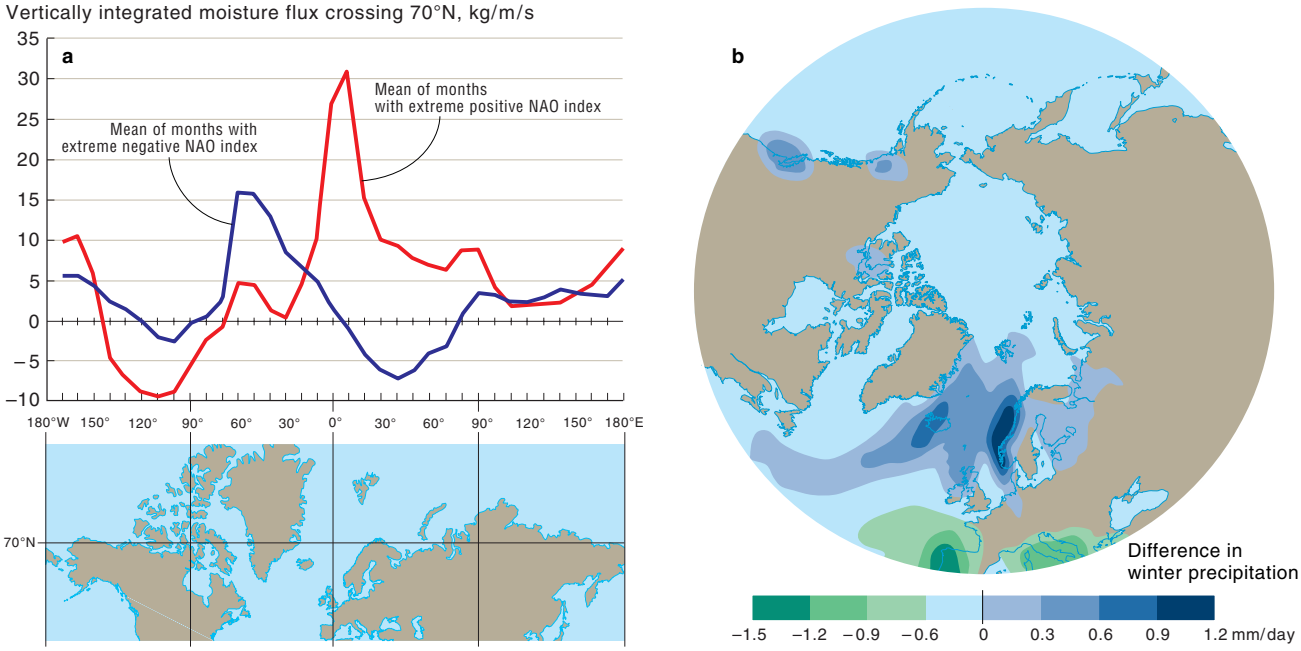

Figure 3·4. The effect of the North Atlantic Oscillation/Arctic Oscillation on precipitation in the Arctic; the NAO and AO are highly correlated and this figure is based on the NAO for which a longer time series exists. The figure illustrates a) the mean vertically integrated meridional flux crossing 70°N in winter for extreme NAO⁻ conditions (blue) and extreme NAO⁺ conditions (red) and b) the change in winter precipitation between extreme NAO⁻ and extreme NAO⁺ conditions (modified from Dickson *et al.*, 2000).

reze *et al.*, 2000; Walsh, 2000). The composite difference in precipitation (Figure 3·4 b), which may actually underestimate the change between index extremes (Dickson *et al.*, 2000), shows an increase of up to 15 cm/yr precipitation during winter in the Norwegian–Greenland Sea atmosphere–ocean conduit to the Arctic when the NAO is strongly positive. The response over the central Arctic to changes in the AO/NAO index is clearly much less, but it is likely that conditions there become wetter during index highs (Serreze *et al.*, 2000). Overall, it is estimated that P–E north of 70°N is 36% higher during periods of high index compared to low index (Serreze *et al.*, 1995). Over central and northern Canada, flux of moisture out of the Arctic increases when the AO/NAO is high, but toward the western Beaufort Sea moisture flux into the Arctic again increases (Figure 3·4 a).

Whether precipitation falls as snow or as rain, and how long snow covers surfaces are important components of climate that control the interaction of contaminants with the hydrological cycle (Macdonald *et al.*, 2002c; Wania, 1997). Snow cover in the Arctic varies from a maximum of about 46×10^6 km^2 to as little as 4×10^6 km^2 (Serreze *et al.*, 2000). As might be predicted from recent warming trends over Arctic land masses (Figure 3·3 a), there is evidence that the average area covered by snow has been decreasing by about 2% (450 000 km^2) per decade between 1979 and 1999 (Armstrong and Brodzik, 2001). A correlation between the AO and snow cover in Eurasia for the period from 1972 to 1997 suggests that a change from minimum to maximum AO index is accompanied by a loss of about 4×10^6 km^2 of snow cover, which could account for much of the trend described above (Vörösmarty *et al.*, 2001). The snow-cover anomalies plotted by Armstrong and Brodzik (2001) show a downward step around 1989 when the AO index sharply increased. The late 1980s up to at least 1998 has been identified as a period of low snow cover for both Eurasia and North America with the largest changes occurring in spring–summer (Serreze *et al.*, 2000); for Canada, there has been a decrease in snow depth, especially in spring, since 1946 (Brown and Goodison, 1996).

Precipitation minus evaporation integrated over a drainage basin should be equivalent to river discharge for the basin (if changes in groundwater or glacial storage are ignored). Arctic rivers exhibit large interannual variation (Semiletov *et al.*, 2000; Shiklomanov *et al.*, 2000; Stewart, 2000) making it difficult to link river flow to precipitation or temperature trends or to climatic variables such as the AO. For example, Shiklomanov *et al.* (2000) suggested little change in mean annual discharge for Arctic rivers between the 1920s and 1990s, whereas Semiletov *et al.* (2000) found recent increases for several Eurasian rivers, and Lammers *et al.* (2001) found evidence of increased winter discharge from rivers in Siberia and Alaska in the 1980s relative to the 1960s and 1970s. Within Can-

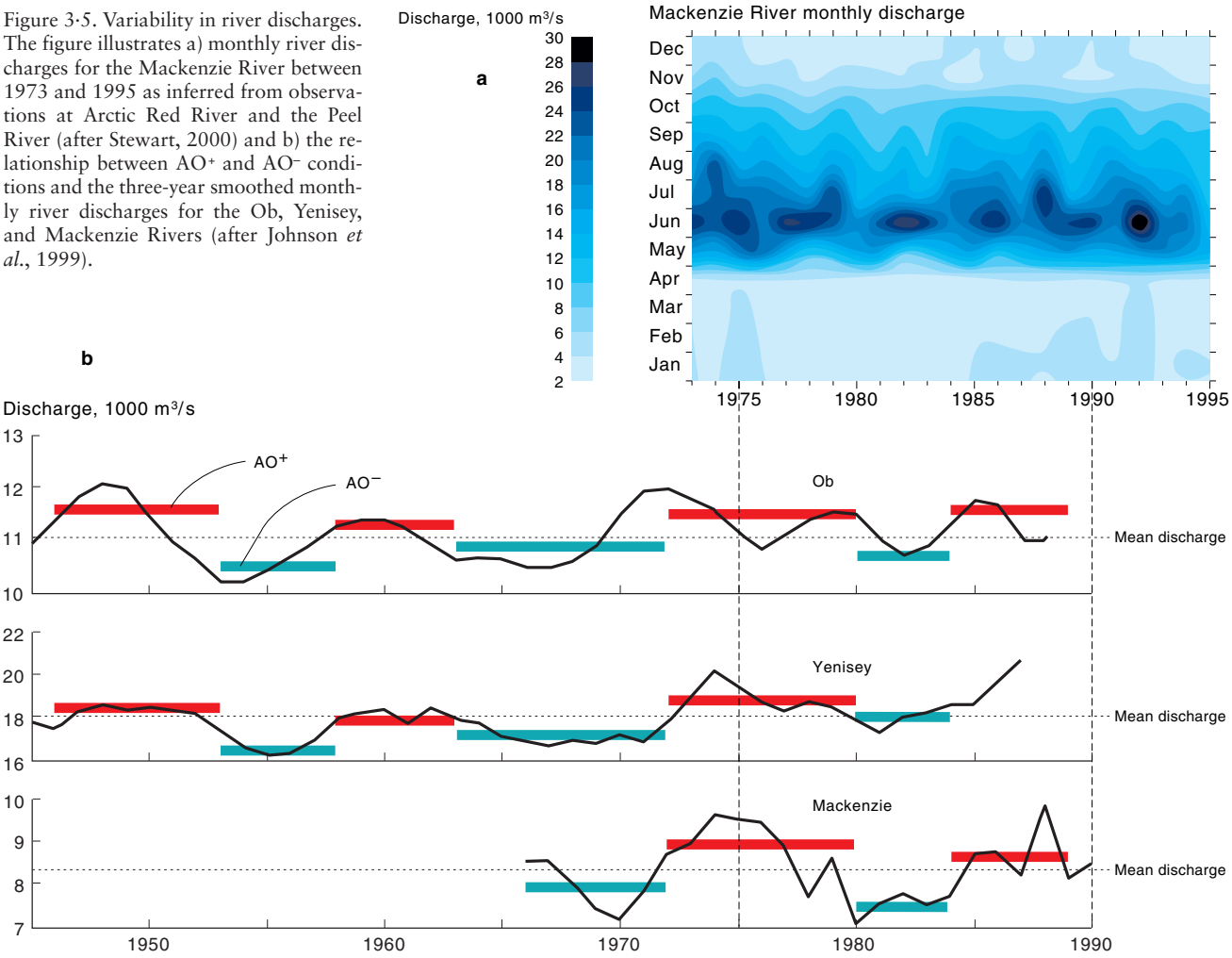

Figure 3·5. Variability in river discharges. The figure illustrates a) monthly river discharges for the Mackenzie River between 1973 and 1995 as inferred from observations at Arctic Red River and the Peel River (after Stewart, 2000) and b) the relationship between AO$^+$ and AO$^-$ conditions and the three-year smoothed monthly river discharges for the Ob, Yenisey, and Mackenzie Rivers (after Johnson *et al.*, 1999).

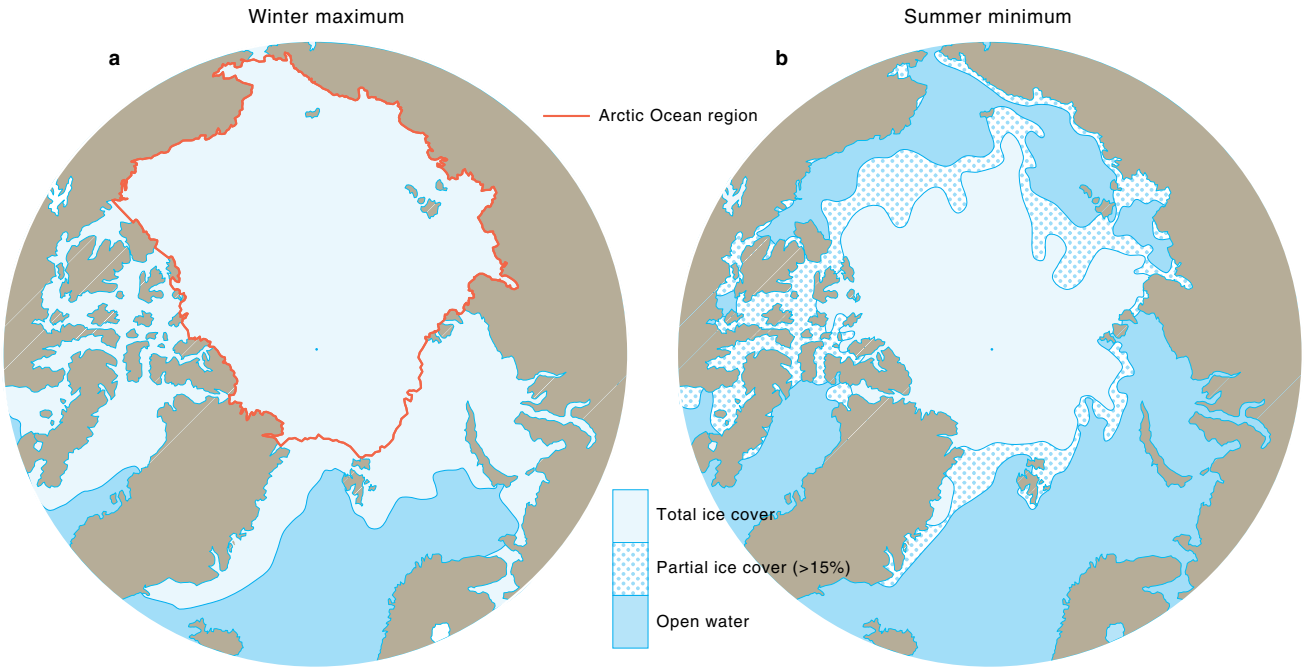

Figure 3·6. Arctic sea-ice cover derived from satellite imagery at the time of a) the winter maximum and b) the summer minimum (Johannessen and Miles, 2000). The red line delimits the Arctic Ocean area as defined for the ice trends shown in Figure 3·7 (Parkinson *et al.*, 1999).

ada, the Mackenzie Basin has undergone an exceptional warming between 1961 and 1990 (Figure 3·3 a); nevertheless, increased basin temperatures are not obviously evident in this river's hydrology (Figure 3·5 a) or in other Arctic rivers (Shiklomanov *et al.*, 2000). Instead, there is evidence of 3- to 4-year periodicity in peak flow and alterations in the seasonal shape of the hydrograph with higher flows delayed well into August, suggesting changes in both total annual discharge and its seasonality and possibly also changes in the relative importance of the river's sub-drainage basins. Such patterns appear to be only partially related to the AO, as evidenced by significant correlations between runoff and precipitation for the Mackenzie Basin and variation in North Pacific storm tracks (Bjornsson *et al.*, 1995). These correlations suggest that trans-Pacific transport of airborne contaminants may be the dominant component of contaminant loading for northwestern Canada, which is supported by air monitoring time-series data collected at Tagish in the Yukon (Bailey *et al.*, 2000). Hence, change related to atmospheric contaminant pathways for this region is more likely to come from the North Pacific, and it is possible that such change might be manifested as an alteration in the domains of influence of Pacific air masses versus Eurasian air masses.

Discharges for the Ob, Yenisey, and Mackenzie rivers appear to show a positive relationship with the North Pole pressure anomaly, with a lag in discharge of about 0.5 to 0.7 years (Figure 3·5 b), but such a relationship runs counter to the enhanced precipitation observed during AO+ (cyclonic) conditions (Figure 3·4). Even if all variation in Arctic river discharge at the 4- to 5-year time scale is assigned to shifts in AO/NAO index, the maximum effect on annual flow would be about 5 to 15% which is within the range of interannual variability (for example see Johnson *et al.*, 1999; Semiletov *et al.*, 2000).

3.5. The Arctic Ocean

3.5.1. Sea ice

3.5.1.1. Sea-ice cover

Sea ice controls the exchange of heat and other properties between the atmosphere and the ocean and, together with snow cover, determines the penetration of light into the sea. Ice also provides a surface for particle and snow deposition, a biological habitat above, beneath and within the ice and, when it melts in summer, creates stratification of the upper ocean.

During the 1990s, the science community recognized (with some alarm) that Arctic sea ice had been undergoing retreat over the previous three decades. Observed changes include: a reduction in area covered by sea ice (Johannessen *et al.*, 1999; Levi, 2000; Maslanik *et al.*, 1996; Parkinson *et al.*, 1999; Vinnikov *et al.*, 1999), an increase in the length of the ice-melt season (Rigor *et al.*, 2002; Smith, 1998), a loss of multi-year ice (Johannessen and Miles, 2000), a general decrease in the thickness of ice over the central Arctic Ocean (Rothrock *et al.*, 1999), and an increase of ice melt in the Beaufort Sea (Macdonald *et al.*, 1999a; McPhee *et al.*, 1998).

Analyses of satellite data from 1978 to 1987 indicate a decrease in Arctic sea-ice area of about 2.4% per decade (Gloersen and Campbell, 1991). Subsequent analyses have revised that figure upward to 4% per decade for the period from 1987 to 1994 with an estimated average loss during the entire period (1978 to 1997) of 3% per decade, which corresponds to the disappearance of 0.3×10^6 km^2 per decade of sea ice (Cavalieri *et al.*, 1997; Parkinson *et al.*, 1999). The Siberian shelves contribute significantly to the estimated ice losses. Multiyear ice is apparently being lost at an even greater rate, estimated at 7% per decade, partly replaced by first-year ice (Johannessen and Miles, 2000).

The large seasonal amplitude in area covered by ice (Figure 3·6) makes it difficult to assess trends. Further-

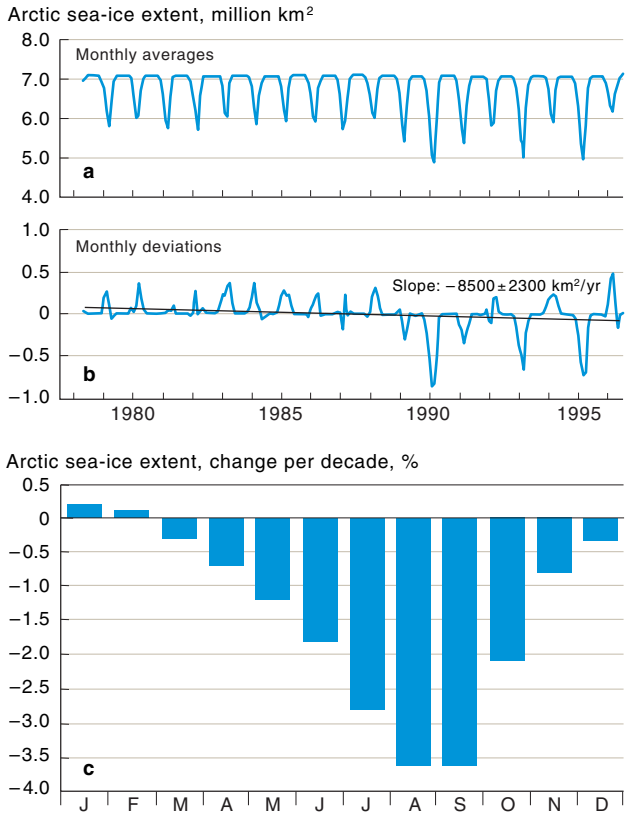

Figure 3·7. Trends in sea-ice cover in the Arctic Ocean. The figure illustrates a) monthly average sea-ice cover between 1979 and 1996 for the Arctic Ocean as delimited by Parkinson *et al.* (1999), see Figure 3·6 a; b) monthly deviations in sea-ice cover for this area showing the transition in 1990 to seasonally clear shelves; and c) the change in monthly sea-ice extent in percent per decade (1979-1995) showing ice loss to be predominantly a spring–summer phenomenon (after Serreze *et al.*, 2000).

more, various authors have partitioned the Arctic differently to assess changes in ice cover or have compared different years and/or different seasons (Dickson *et al.*, 2000; Johannessen and Miles, 2000; Maslanik *et al.*, 1996, 1999; Parkinson *et al.*, 1999). Despite these difficulties, the satellite data available since the late 1970s clearly indicate a reduction of 2% per decade of total ice area in winter (Johannessen *et al.*, 1999), and a significant shift in the marginal seas toward first-year ice which is easier to melt than multi-year ice because it is thinner and saltier. The total area of Arctic sea ice, including the marginal seas, varies from about 13×10^6 km² in winter to 5×10^6 km² in summer, and has shrunk by about 0.6×10^6 km² between 1978 and 1997 (Johannessen and Miles, 2000). The Arctic Ocean component, as defined by Parkinson *et al.* (1999) (Figure 3·7), which is about 7×10^6 km² in area, began to exhibit a much stronger seasonal modulation in ice cover in about 1989 (Figures 3·7 a and b) with the East Siberian and Beaufort Seas experiencing anomalous areas of open water in late summer at various times during the 1990s (Maslanik *et al.*, 1999; Parkinson *et al.*, 1999; Rigor *et al.*, 2002; Serreze *et al.*, 1995). That the loss of sea-ice cover is predominantly a spring–summer phenomenon is clearly shown by seasonal monthly trends for which June to October show the greatest change (Figure 3·7 c; Serreze *et al.*, 2000).

What part does the AO play in the variation of Arctic sea-ice distribution? The trends in ice cover with time (Figures 3·7 a and b) suggest that the wholesale clearing of ice from shelves is a phenomenon of the 1990s, timed with (Russian shelves) or slightly delayed from (Beaufort shelves) the shift to strong AO⁺ conditions in 1989. In the Beaufort Sea, Macdonald *et al.* (1999a) used stable isotope data ($\delta^{18}O$) collected from 1987 to 1997 to show that amounts of ice melt contained in the water column increased substantially at the same time as the AO index increased in 1989. During such conditions, the cyclonic circulation leads to greater ice divergence, more new ice in leads, enhanced heat flux, and reduced ridging, all of which imply thinning (Flato and Boer, 2001; Macdonald *et al.*, 1999a; Rigor *et al.*, 2002). Maslanik *et al.* (1996) draw the connection between increased penetration of cyclones, which is observed during AO⁺ conditions, and increased poleward transport of heat, and the absence of ice in late summer over the Siberian shelves. Based on results of a coupled sea/ice/ocean model, Zhang *et al.* (2000) suggest that there is a strong correlation between sea-ice thinning and the AO (~80%) due to dynamical effects, and that the Eurasian and Canada Basins respond differently to the AO forcing. The removal of the supply of ice from the Beaufort to the East Siberian Sea when the index becomes strongly positive (discussed in section 3.5.1.2.) results in depletion of thick ice in the eastern Arctic Ocean but may enhance thick ice-buildup in the western Arctic. This is important in light of the findings from repeat submarine surveys that ice thickness has decreased over the central Arctic by about 1.3 m between 1958 and 1976 and the 1990s (Rothrock *et al.*, 1999; Wadhams, 1997, 2000). According to several models (Holloway and Sou, 2002; Polyakov and Johnson, 2000; Zhang *et al.*, 2000), the submarine observations may have been conducted primarily in that part of the ocean that underwent thinning in response to a shift to AO⁺ conditions. The conclusion concerning reduction of ice thickness, while valid for the domain of submarine measurements, is not necessarily true for the whole Arctic Ocean and an alternative hypothesis that ice-thickness *distribution* changed but ice *volume* may not have changed in response to the AO needs to be carefully evaluated. The loss of ice cover between NAO⁻

Figure 3·8. The contrast in ice cover between pronounced AO⁻ conditions (1958) and pronounced AO⁺ conditions (1990s) (Dickson *et al.*, 2000; Maslanik *et al.*, 1999; Serreze *et al.*, 1995).

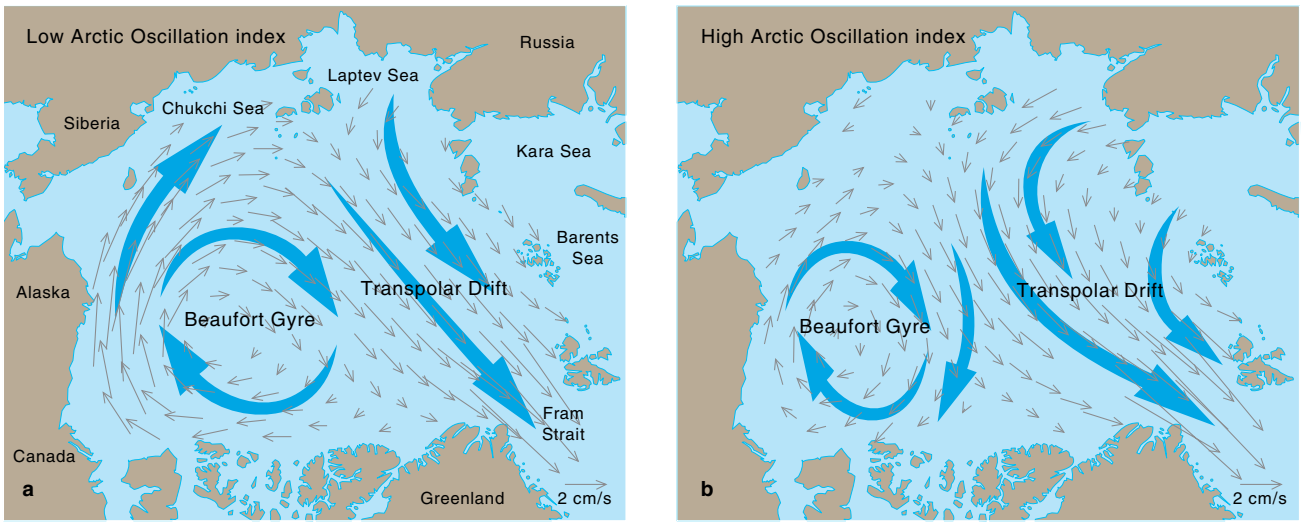

Figure 3·9. Ice drift patterns for a) years with pronounced AO⁻ (anticyclonic) conditions and b) pronounced AO⁺ (cyclonic) conditions (after Maslowski *et al.*, 2000; Polyakov and Johnson, 2000; Rigor *et al.*, 2002). The small arrows show the detailed ice drift trajectories based on an analysis of sea level pressure (Rigor *et al.*, 2002). The large arrows show the general ice drift patterns long recognized as the Beaufort Gyre to the left and the Transpolar Drift to the right.

and NAO⁺ conditions is estimated at 590 000 km^2 in the Barents and Greenland Seas (Dickson *et al.*, 2000), and if the remarkably open ice in the East Siberian Sea in 1990 and the Beaufort Sea in 1998 (Figure 3·8) is a product of the strong AO⁺ conditions of the early 1990s then perhaps half as much again ice loss occurred over the Russian and North American shelves due to AO forcing.

In light of the changes observed in ice cover during the 1990s, it is worth noting that over a century ago the Pacific whaling fleet experienced similar dramatic changes in ice conditions in the western Arctic. Extraordinarily open water from 1861 to 1867 may have contributed to a complacency that resulted in the loss of 32 ships, crushed in the ice along the Alaskan coast in 1871 (Bockstoce, 1986). In this respect it is interesting to remember the caution given by Polyakov and Johnson (2000), that both short (decadal) and long (60-80 yr) time-scale variations are associated with the AO.

From data collected between 1979 and 1997, Rigor *et al.* (2000) determined that sea-ice melt begins in the marginal seas by the first week of June and advances rapidly to the pole within two weeks. Freezing begins at the pole on 16 August, returning to the marginal seas by late September for a total melt season length of about 58 days at the pole and 100 days toward the margin. Based on satellite data (SSMR and SSM/I) predominantly from the Beaufort Sea, Smith (1998) estimated that the length of the melt season has been increasing by about 5.3 days per decade during the period 1979 to 1996. In contrast, Rigor *et al.* (2000) found a shortening of the melt season in the western Arctic of 0.4 days per decade and an increase of about 2.6 days per decade in the eastern Arctic. These trends in length of melt season parallel the general observations of a 1°C per decade *decrease* in temperature for the Beaufort Sea compared to a 1°C per decade *increase* in the eastern Arctic for the same time period (Rigor *et al.*, 2000).

Change in ice cover and its seasonality are especially important for contaminants like hexachlorocyclohexanes (HCHs), toxaphene, and polychlorinated biphenyls (PCBs) where air–sea exchange is a significant component of regional budgets (Macdonald *et al.*, 2000a,b). Furthermore, change in sea-ice cover, which alters light penetration and mixing, may also alter primary production and carbon flux (Gobeil *et al.*, 2001b) which then alters the vertical flux of particle reactive and bio-active contaminants from the ocean surface to depth.

3.5.1.2. Sea-ice drift

General ice motion in the Arctic Ocean follows the Transpolar Drift (TPD) on the Eurasian side of the ocean and the Beaufort Gyre in Canada Basin (Figure 1·1; Barrie *et al.*, 1998). Although it has long been recognized that large-scale ice-drift patterns in the Arctic undergo change (Gudkovich, 1961), it was not until the International Arctic Buoy Programme (IABP) that sufficient data became available to map the ice drift in detail and thereby directly evaluate the role of the AO in changing ice drift trajectories. The IABP data from 1979 to 1998 suggest two characteristic modes of Arctic ice motion, one during low index (AO⁻) and the other during high index (AO⁺) periods (Figures 3·9 a and b; Proshutinsky and Johnson, 1997; Rigor *et al.*, 2002). The ice-motion scheme shown by drifting buoys is reasonably well corroborated by models that are being used to investigate the influence of the atmospheric variability inherent in the AO (Maslowski *et al.*, 2000; Polyakov and Johnson, 2000). There are two overarching differences between the two ice circulation modes:

1) during AO⁻ conditions (Figure 3·9 a), ice in the TPD tends to move directly from the Laptev Sea across the Eurasian Basin and out into the Greenland Sea, whereas during strong AO⁺ conditions (Figure 3·9 b) ice in the TPD takes a strong cyclonic diversion across the Lomonosov Ridge and into Canada Basin (Mysak, 2001); and

2) during AO⁺ conditions (Figure 3·9 b), the Beaufort Gyre shrinks back into the Beaufort Sea and becomes more disconnected from the rest of the Arctic Ocean, exporting less ice to the East Siberian Sea and importing little ice from the region to the north of the Canadian Arctic Archipelago – a region known to contain the Arctic's thickest multi-year ice (Bourke and Garrett, 1987).

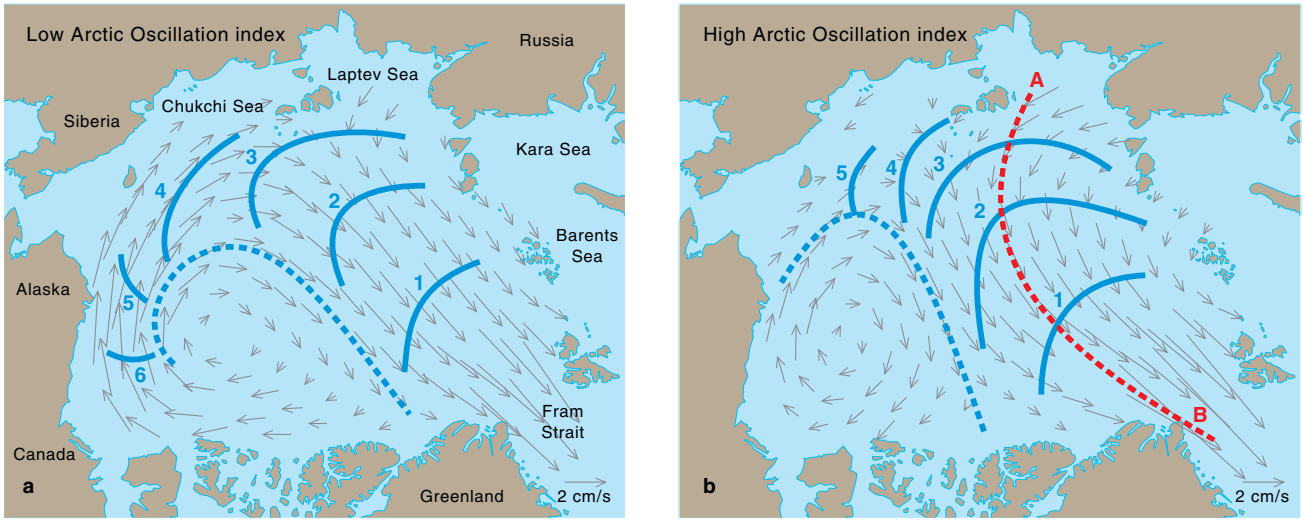

Figure 3·10. Time taken in years for sea ice at that location to reach Fram Strait during a) pronounced AO⁻ conditions and b) pronounced AO⁺ conditions (after Rigor *et al.*, 2002). Line A-B represents the transect used to describe change in sea ice during drift shown in Figure 3·12.

There are also changes in the time required for ice to transit the ocean (Figures 3·10 a and b) and in the destinations of ice exported from shelves. During winter, under AO⁺ conditions there is an increase in ice advection away from the East Siberian and Laptev Sea coasts, leading to the production of more new, thin ice in the coastal flaw leads (Figure 3·11; Polyakov and Johnson, 2000; Rigor *et al.*, 2002), a decrease in the advection of ice from the western Arctic into the eastern Arctic, possibly an increased advection of ice from the Arctic Ocean to the Barents Sea through the Svalbard–Franz Josef Land passage (Polyakov and Johnson, 2000), and an increase in the 900 000 km^2 of ice advected out of the Arctic through Fram Strait (Morison *et al.*, 2000; Rigor *et al.*, 2002). Interestingly, increased ice export through Fram Strait can be produced by shifts to both negative and positive AO states (Dickson *et al.*, 2000).

Comparing the two modes of ice drift (Figures 3·9 a and b), it is apparent that during AO⁻ conditions the East Siberian Sea imports much of its ice from the Beaufort Sea and that there is an efficient route to carry ice clockwise around the Arctic margin of the East Siberian Sea and out toward Fram Strait. Under the strong AO⁺ conditions of the early 1990s, the Beaufort Sea ice be-

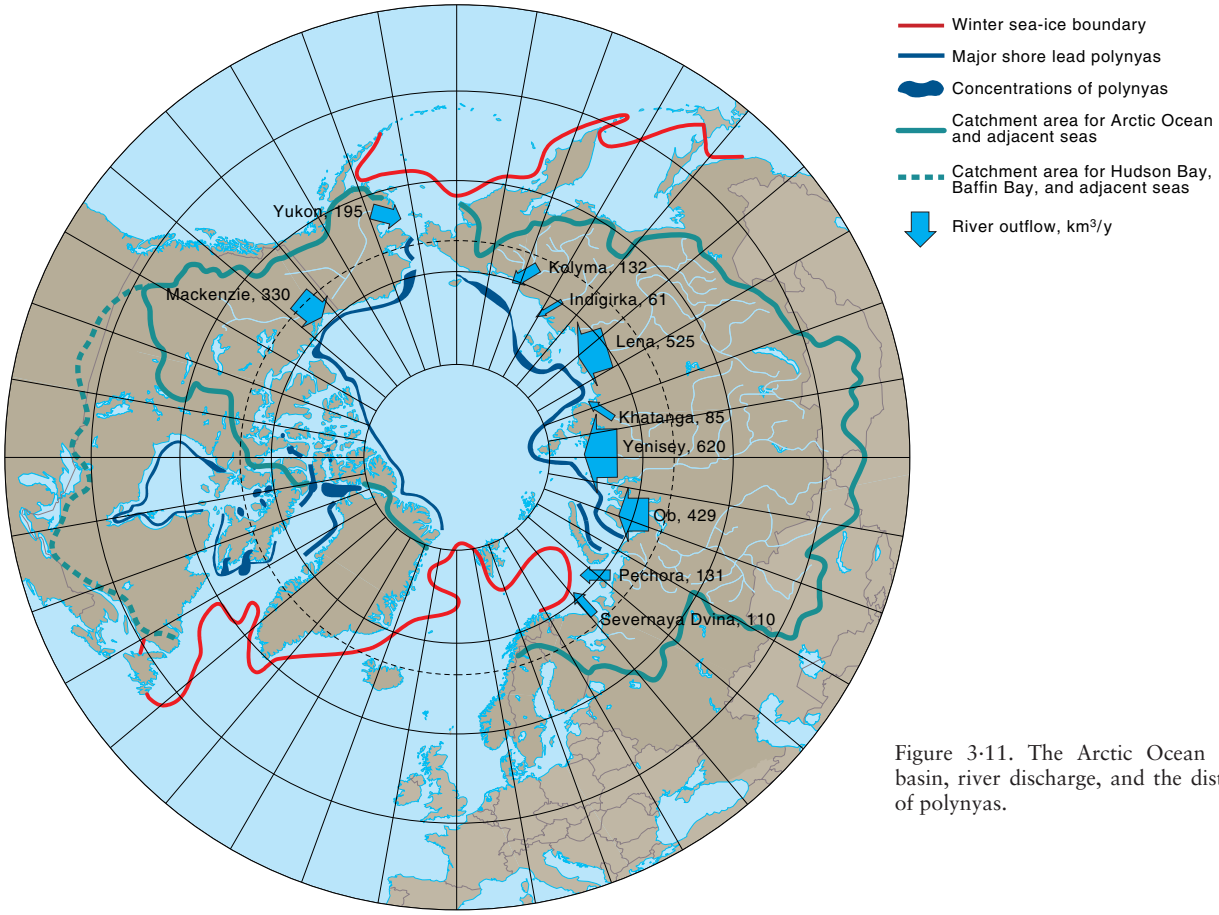

Figure 3·11. The Arctic Ocean drainage basin, river discharge, and the distribution of polynyas.

came more isolated, whereas ice from the Kara, Laptev and East Siberian Seas was displaced into the central Arctic and toward the Canadian Arctic Archipelago. It is not clear from the IABP data how much ice from the Russian shelves might transport into the Canadian Arctic Archipelago or the Beaufort Gyre under AO⁺ conditions, but models (Maslowski *et al.*, 2000; Polyakov and Johnson, 2000), paleo-studies of Eurasian wood (Dyke *et al.*, 1997; Tremblay *et al.*, 1997), and sediment records (Darby *et al.*, 2001) all suggest that such transport is likely and may at times be important.

Sea ice provides a rapid means to accumulate and transport contaminants long distances without dilution (Pfirman *et al.*, 1995; Wadhams, 2000). The response in ice-drift trajectories to change in AO index (Rigor *et al.*, 2002) therefore carries immense implication for the connectivity between contaminant source and sink regions for ice pathways within the Arctic Ocean.

3.5.1.3. Sea-ice transport of material

Sea ice is an important mechanism for the transport of coastal and continental shelf sediments to the interior Arctic Ocean and out into the Greenland Sea (Barrie *et al.*, 1998; Dethleff *et al.*, 2000b; Nürnberg *et al.*, 1994). Sediments become incorporated into ice formed over shelves. Although all the shelves of the Arctic are implicated in this process, the Laptev Sea has proven so far to be the most efficient exporter of sediment-laden ice (Eicken *et al.*, 1997, 2000; Reimnitz *et al.*, 1992, 1993, 1994). This transport process involves several steps including: 1) the delivery of sediment to the shelf by rivers or from coastal erosion where much of it may become trapped; 2) the incorporation of sediment into the ice, either through ice grounding or through suspension freezing in mid-shelf flaw polynyas; 3) the export of ice from the shelf to the interior ocean; 4) the transport of ice across Arctic basins, potentially with some loss of sediment during transport; and 5) the release of sediment at the location where the ice melts (Figure 3·12). During transport, the ice 'weathers', ablating at the surface during summer and incorporating more ice on the bottom during winter, with the consequence that some of the sediment entrained over the shelf migrates to the surface of the ice. Additionally, atmospheric particulates deposit and accumulate on the ice along its transport route. Consequently, an increase or decrease in the time taken for ice to cross the Arctic Ocean (Figure 3·10) respectively increases or decreases the time for accumulation of atmospheric aerosols and sediments at the ice surface. Each step in the ice pathway can be altered by climate change. For example, fine river sediments (known to carry contaminants) become trapped in estuaries by the so-called 'marginal filter' (Lisitzin, 1995). Sea level rise, change in the ice climate, or change in the river's hydrology can all alter the location of this filter. The process of suspension freezing might be enhanced by larger amounts of open water over shelves in the autumn whereas more sediment might be lost from the ice during transport due to predominance of thin, first-year ice and augmented melting. Finally, the location at which ice melts and drops its particulate and dissolved loads can change. There are no direct data on how these components of the ice-transport pathway respond either individually or collectively to the AO; however, long-term sediment records (Darby *et al.*, 2001), disequilibria in sediments (Gobeil *et al.*, 2001b), and the distribution of sediments within the Arctic Ocean (Stein, 2000) suggest that climate forcing akin to the AO probably occurs.

3.5.2. Ocean currents and water properties

3.5.2.1. Surface water

For ocean currents that deliver contaminants to Arctic ecosystems, surface water is most important because it interacts more directly with biota and ecosystems. Surface water pathways will to some extent reflect ice-drift trajectories (Morison *et al.*, 2000), responding in like manner to the state of the AO (Figure 3·9). In strong AO⁺ conditions, water in the TPD makes a diversion into the Makarov Basin and the Beaufort Gyre contracts and retreats into Canada Basin. However, the AO results in other critical changes in surface water not represented by ice drift. With the enhanced inflow and spreading of water in the Atlantic Layer, a retreat of the cold halocline in the Eurasian Basin under AO⁺ conditions was also

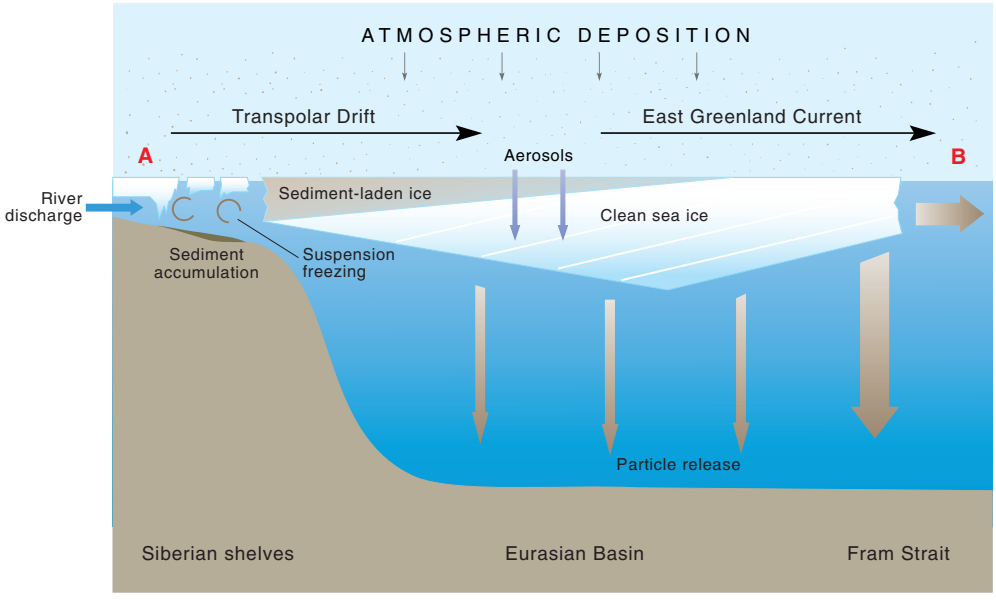

Figure 3·12. A schematic diagram showing the accumulation and transport of sediments and contaminants by sea ice over the transect marked A-B on Figure 3·10 b (modified from Lange and Pfirman, 1998).

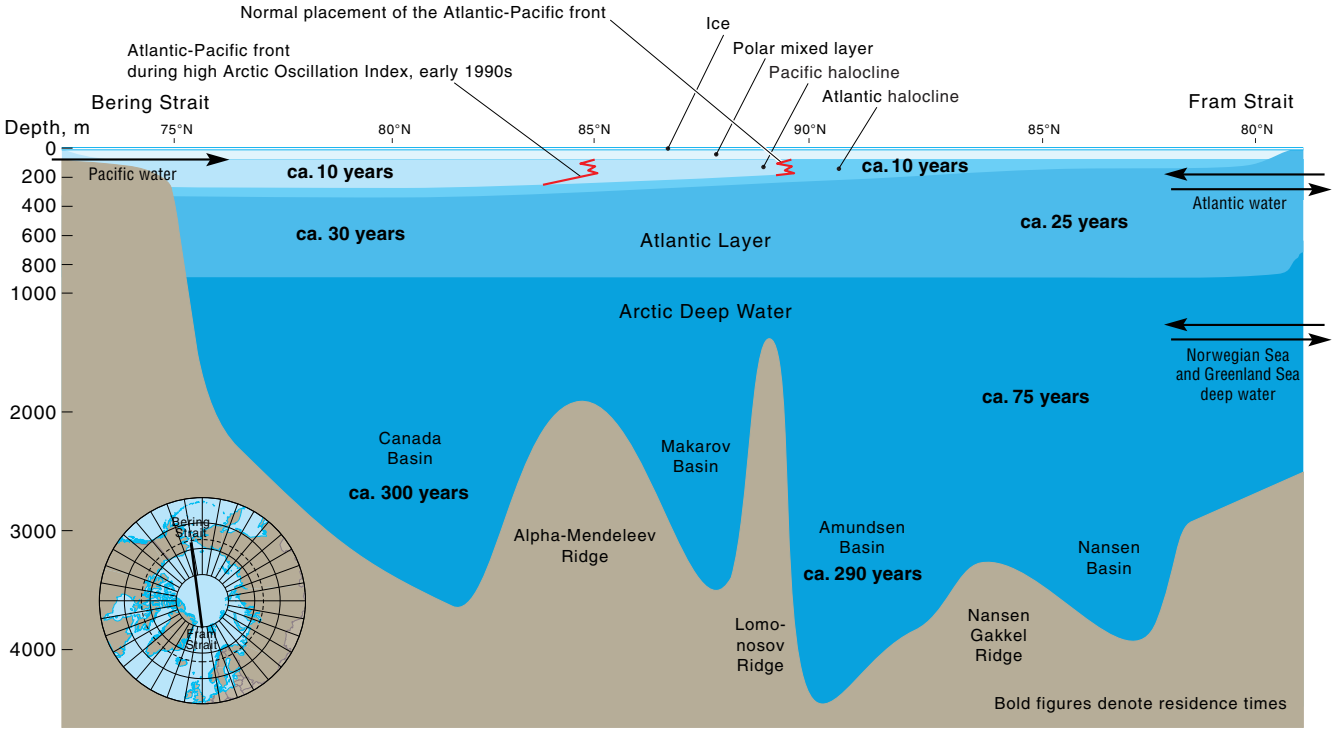

Figure 3·13. The stratification of the Arctic Ocean, showing the polar mixed layer, the Pacific and Atlantic domains of influence and the haloclines. The red lines show the normal placement and the displacement of the Atlantic-Pacific front during the high Arctic Oscillation index of the early 1990s.

noted (Steele and Boyd, 1998). The halocline (Figure 3·13) provides stratification between the Atlantic Layer and surface water thereby preventing or reducing the transfer of properties such as heat or contaminants between deep and surface layers. The increase in salinity of surface water in the Eurasian Basin noted by Steele and Boyd (1998), however, was not due to enhanced inflow from the Atlantic, which actually freshened slightly with the high AO/NAO index of the late 1980s, but rather to the diversion of river inflow at the margins of the Arctic Ocean.

Models (Figures 3·14 a and b; Dickson, 1999; Johnson and Polyakov, 2001; Maslowski *et al.*, 1998) and geochemical measurements (Ekwurzel *et al.*, 2001; Guay *et al.*, 2001; Macdonald *et al.*, 1999a, 2002a; Schlosser *et al.*, 2002) clearly show that with the high AO⁺ index of the late 1980s, river water entering the Laptev and Kara shelves was forced to the east rather than directly off the shelf and into the TPD. Under strong AO⁺ conditions, perhaps 1000 km³/yr or more of runoff from the Lena, Ob, and Yenisey rivers stopped entering the Eurasian Basin and entered, instead, the East Siberian shelf and thence the Canadian Basin, possibly to exit the Arctic Ocean via the Canadian Arctic Archipelago (Figures 3·14 c and d) (Morison *et al.*, 2000). A consequence of this diversion was a reduction of stratification in the Eurasian Basin (Steele and Boyd, 1998) and an increase in stratification in the Canadian Basin (Macdonald *et al.*, 1999a, 2002a). The drop in the AO index toward the end of the 1990s (Figure 3·1) appears to have initiated a return to the former pathways for river water in the Eurasian Basin (Björk *et al.*, 2002; Boyd *et al.*, 2002).

At the same time, Atlantic surface water invaded the Makarov Basin, displacing water of Pacific origin from the top 200 m of the water column (McLaughlin *et al.*, 1996); this represents a rapid change of water source and properties for about 20% of the Arctic Ocean's area (Figures 3·13 and 3·15). Although there does not appear to be a strong AO signal in the Pacific inflow through Bering Strait (~0.8 Sv, there has been a general decline of about 15% since the early 1940s (Coachman and Aagaard, 1988; Roach *et al.*, 1995) and the flow may also have freshened due to runoff and precipitation in the Bering Sea (Weingartner, pers. comm., 2001).

3.5.2.2. The Atlantic Layer

Repeat hydrographic surveys of Arctic basins, commencing in 1987 (Aagaard *et al.*, 1996; Anderson *et al.* 1989; Carmack *et al.*, 1995; McLaughlin *et al.*, 1996; Morison *et al.*, 1998; Quadfasel *et al.*, 1991; Swift *et al.*, 1997), have revealed an Arctic Ocean in transition. The timing of that transition in the late 1980s implicates the AO (or NAO) as a major source of forcing that has altered connections between the Atlantic and the Arctic Oceans and so changed the distribution of Atlantic water within the Arctic, both in the surface layer, as discussed in section 3.5.2.1, and in the deeper Atlantic Layer water (Dickson, 1999; Macdonald, 1996). Ironically, some of the clearest evidence of these changes has come from contaminant time series, in particular the tracing of artificial radionuclides released from European reprocessing plants into the waters of the eastern North Atlantic (Carmack *et al.*, 1997; Smith *et al.*, 1998).

A major change, starting in about 1989, was a possible intensification of flow from the Atlantic into the Arctic through Fram Strait and the Barents Sea in response to the shift to strong AO⁺ or NAO⁺ conditions (Figure 3·15 – for detailed reviews see Dickson *et al.*, 2000; Morison *et al.*, 2000; Serreze *et al.*, 2000). The winds associated with AO⁺ conditions (Figure 3·2) increased the rate of northward transport of surface water in the Norwegian Sea and produced warmer air temperatures,

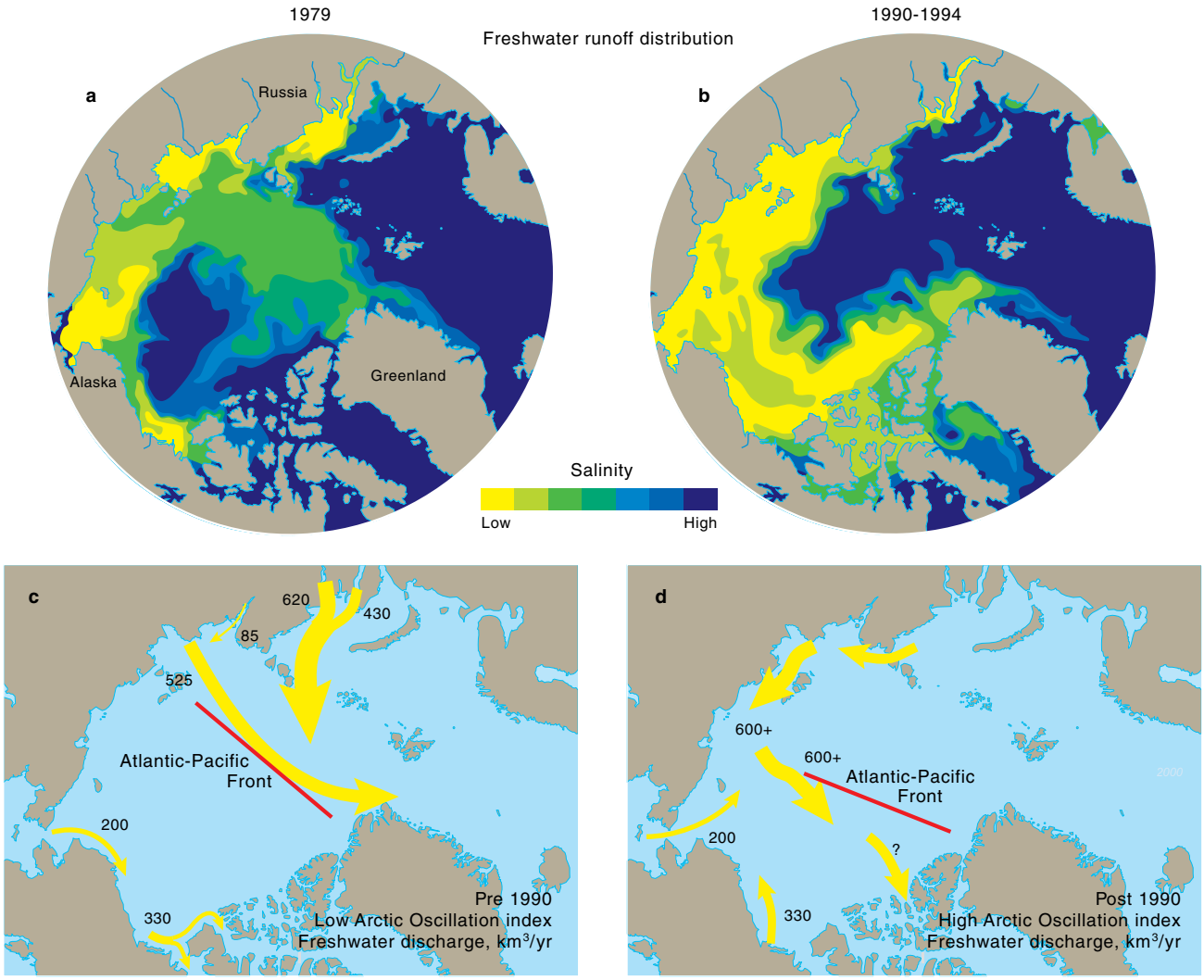

Figure 3·14. Transport of freshwater runoff across the Arctic Ocean. This figure illustrates a) freshwater pathways during pronounced AO⁻ conditions (1979); b) freshwater pathways during pronounced AO⁺ conditions (1990-94) (both a and b are based on model results by W. Maslowski reproduced in Dickson, 1999); c) the amounts and changes in pathways for freshwater inflows during AO⁻ conditions; and d) the amounts and changes in pathways for freshwater inflows during AO⁺ conditions.

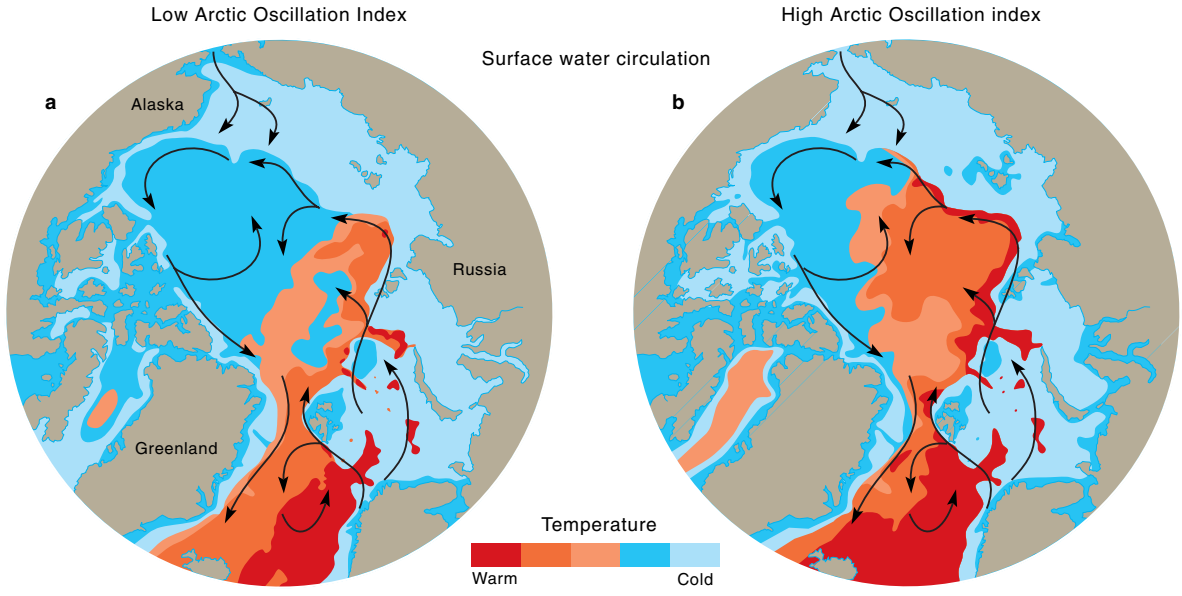

Figure 3·15. The change in Atlantic water inflow to the Arctic and distribution within the Arctic produced by the exceptionally strong shift to AO⁺/NAO⁺ conditions around 1989. The figure illustrates a) the distribution of Atlantic Layer water prior to the late 1980s and b) the distribution of Atlantic Layer water during the early to mid 1990s. The distribution of the Atlantic Layer (see Figure 3·13) is based on Hodges (2000), Maslowski *et al.* (2000), McLaughlin *et al.* (1996), and Morison *et al.* (1998, 2000). The Atlantic Layer boundary currents, which are relatively fast, transport properties along basin margins at about 1-5 cm/s (300-1600 km/yr; Woodgate *et al.*, 2001).

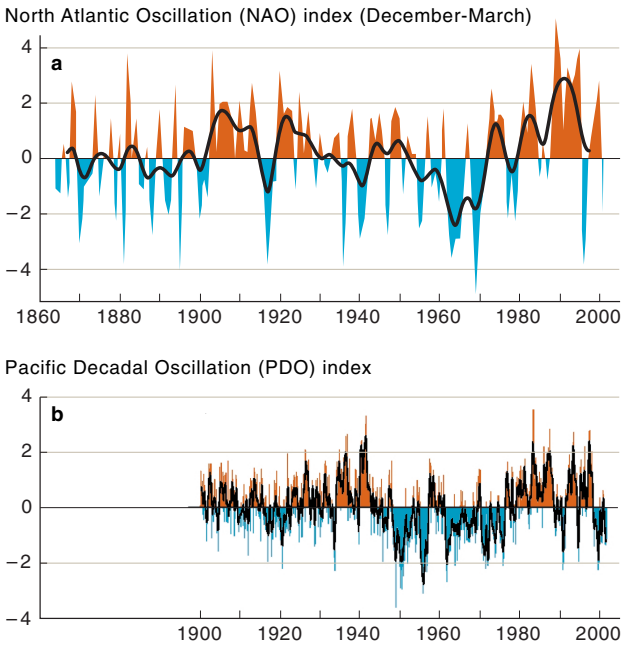

Figure 3·16. a) The North Atlantic Oscillation index from 1860 to 2000 (source: Hurrell, 2002) and b) the Pacific Decadal Oscillation index 1900 to 2000.

which, together with the shorter transit times, contributed to warming by about 2.3°C of the Atlantic water entering the Arctic Ocean (Swift *et al.*, 1997). The Atlantic water also exhibited slightly decreased salinity (by 0.03-0.05), probably reflecting increased precipitation in the Nordic Seas during NAO⁺ conditions (Figure 3·4 b).

Within the Arctic Ocean, the changes in the distribution and composition of the Atlantic Layer water were spectacular when set against the traditional perception of a quiet, steady-state ocean (see Figures 3·13 and 3·15 for the position of the Atlantic Layer within the water column). The front between Atlantic water and Pacific water, traditionally located over the Lomonosov Ridge was forced over to the Alpha-Mendeleev Ridge (Figure 3·13 and see McLaughlin *et al.*, 1996; Morison *et al.*, 2000). At the same time, the inflowing water could be detected in the Atlantic Layer by an approximately 1.5°C temperature rise above the climatological norm (Carmack *et al.*, 1995). The changes in volume and composition of Atlantic water entering the Arctic Ocean through Fram Strait continue to cascade through the Arctic basins, first as changes in properties along the boundaries (McLaughlin *et al.*, 2002; Newton and Sotirin, 1997), then as changes propagated into the basin interiors along surfaces of constant density (Carmack *et al.*, 1997) (Figure 3·13). Woodgate *et al.* (2001) estimated that in 1995 to1996, the boundary flow over the southern margin of the Eurasian Basin was transporting 5±1 Sv at about 1 to 5 cm/s (300-1600 km/yr). When water in the boundary current reached the Lomonosov Ridge, the flow split with around half entering the Canadian Basin along its margin and half returning toward Fram Strait along the Lomonosov Ridge. The high NAO index of the late 1980s (Figure 3·16 a) also strengthened and warmed the inflowing Barents Sea branch of Atlantic water, perhaps by as much as 25% relative to 1970 (Dickson *et al.*, 2000), which probably led to a parallel warming and increase in salinity of the Barents Sea (Zhang *et al.*, 2000).

3.6. Adjacent polar seas and regions

3.6.1. The Nordic and Barents Seas

The Nordic Seas (Greenland, Iceland and Norwegian Seas) are dominated by a northward flow of warm Atlantic water on the eastern side and a southward flow of cold Arctic water on the western side (Figure 3·17). The northward flows are large, estimated at 7 to 8 Sv in the Norwegian Atlantic Current (NwAC). About 2 Sv of the NwAC enters the Barents Sea and the remainder continues north where part enters the Arctic Ocean through Fram Strait and part re-circulates toward the west (Barrie *et al.*, 1998; Dickson *et al.*, 2000).

The currents that transport warm Atlantic water to the Barents Sea are important for regional climate, keeping the entire Norwegian Sea and large areas of the Barents Sea ice free and open for biological production. These same currents provide a significant pathway for contaminants from the western coast of Europe and perhaps from as far as the eastern North American seaboard. The volume flux for these currents and the distribution of Atlantic water in the Norwegian Sea is strongly influenced by wind forcing (e.g., Blindheim *et al.*, 2000; Hansen *et al.*, 2001; Mork and Blindheim, 2000; Orvik *et al.*, 2001), with a large component of variation accounted for by the NAO index (Figure 3·17).

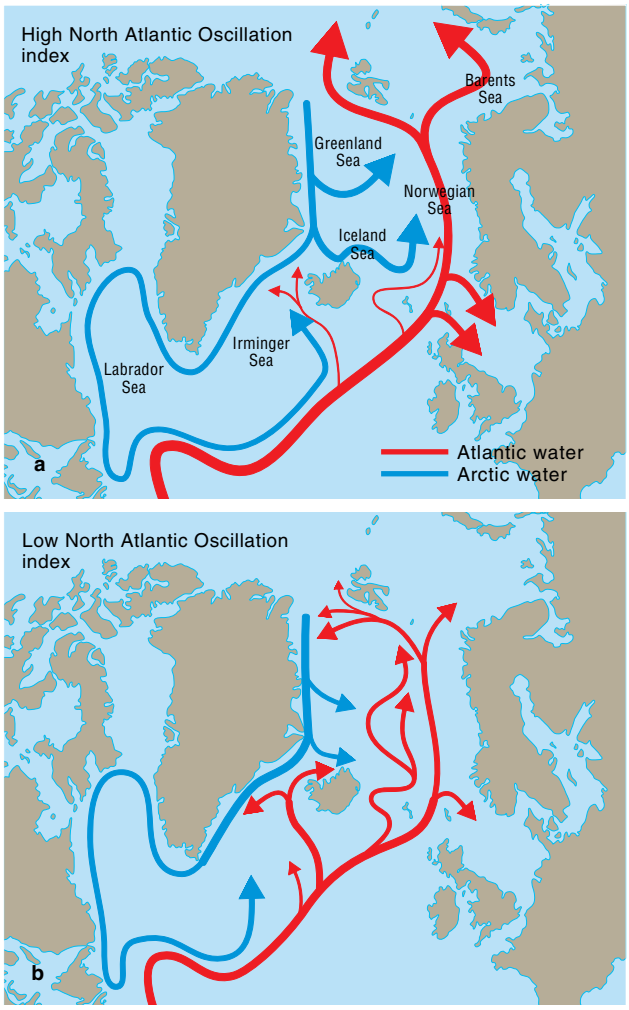

Figure 3·17. Main features of the circulation of Atlantic waters (red) and Arctic waters (blue) in the northern North Atlantic and Nordic Seas under a) pronounced NAO⁺ conditions and b) pronounced NAO⁻ conditions (source: Blindheim *et al.*, 2000).

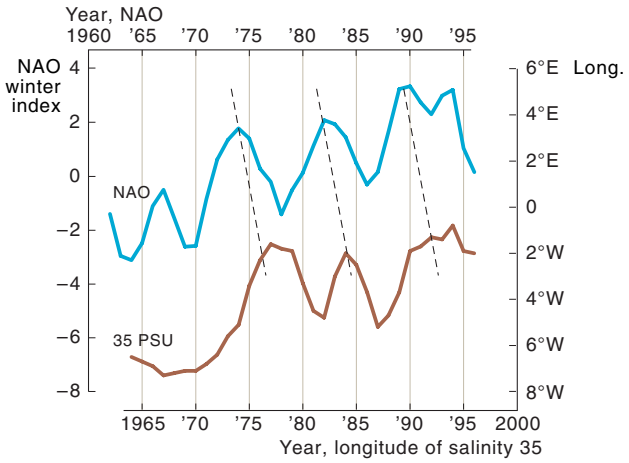

Figure 3·18. A comparison of the western extent of Atlantic Water (brown curve) and the NAO index (blue curve). The brown curve reflects three-year moving averages of the longitude of maximum western extent of water with salinity of 35 in the section along 65°45'N (source: Blindheim *et al.*, 2000). The blue curve reflects a three-year moving average of NAO winter values (Dec-March) (updated from Hurrell, 1995). The two lines are strongly correlated with a time-lag of ca. 2-3 years between respective peaks.

A high winter NAO index (December-March) is associated with more south-westerly winds and storms which increase the volume flux of the inner (eastern) branch of the NwAC (compare Figure 3·17a with Figure 3·17b; Orvik *et al.*, 2001). Under these conditions, more Atlantic water reaches the Barents Sea and the Arctic Ocean, and less Atlantic water is transported into the central Norwegian Sea (Blindheim *et al.*, 2000). Coincidentally, more Arctic water from the East Greenland Current, which is fresher and cooler, enters the central Norwegian Sea. During periods of low NAO index (Figure 3·17b), weaker south-westerlies result in a weaker inner branch of the NwAC and a greater extension of Atlantic water to the west in the Norwegian Sea. The east–west extent of Atlantic water passing through the Norwegian Sea predictably follows the winter NAO index with a lag of 2 to 3 years (Figure 3·18).

Large-scale atmospheric features, as represented by the NAO, appear to affect the strength of the Atlantic inflow to the Barents Sea (Figure 3·17; Dippner and Ottersen, 2001; Ingvaldsen *et al.*, 2002) but this inflow seems also to be closely related to regional atmospheric circulation (Ådlandsvik and Loeng, 1991). Low atmospheric pressure over the inflow area favours increased inflow of Atlantic water resulting in higher than average temperatures in the Barents Sea.

From the mid-1960s the NAO index has increased progressively with relatively high values in the early- to mid-1990s (Figure 3·16a). Increased atmospheric carbon dioxide (CO_2) is projected to increase storm frequencies and weaken thermohaline circulation (IPCC, 2002) probably producing upper ocean circulation more like that observed during NAO+ conditions (Figure 3·17a). The increased wind-induced transport may be partly compensated for by a reduced thermohaline circulation with the net effect of a relatively large transport of Atlantic water to the Barents Sea and the Arctic Ocean, and increased influence of Arctic water masses on the western and central Norwegian Seas.

Vertical mixing of water masses is important for biological production and for redistribution of contaminants. In the Greenland Sea, deep or intermediate water masses are created by winter cooling of the upper layer, a process which has weakened or even ceased since the beginning of the 1970s (e.g., Bönisch *et al.*, 1997). In the Barents Sea, vertical mixing takes place down to 300 m in cold years, which means the whole water column is well mixed from the surface to the bottom. In addition to vertical mixing due to cooling in the open sea, vertical mixing also takes place in frontal zones of the Nordic and Barents Seas. Cold and warm water masses meet and mix to create a very productive area where there is likely to be a high organic sedimentation rate. The fronts also act as a barrier for distribution of both plankton and fish.

3.6.2. The Bering and Chukchi Seas

The eastern Bering and Chukchi Seas are contiguous shelves that extend nearly 2000 km northward from the Alaskan Peninsula to the continental slope of the Arctic Ocean's Canada Basin (Figure 3·19). Both shelves are broad and shallow with typical depths on the Bering and Chukchi shelves being <100m and <60m, respectively. The Bering Strait provides a continuous pathway by which approximately 25 000 km^3 of water from the North Pacific Ocean enter the Arctic Ocean annually (Roach *et al.*, 1995). The nutrient-rich, but moderately

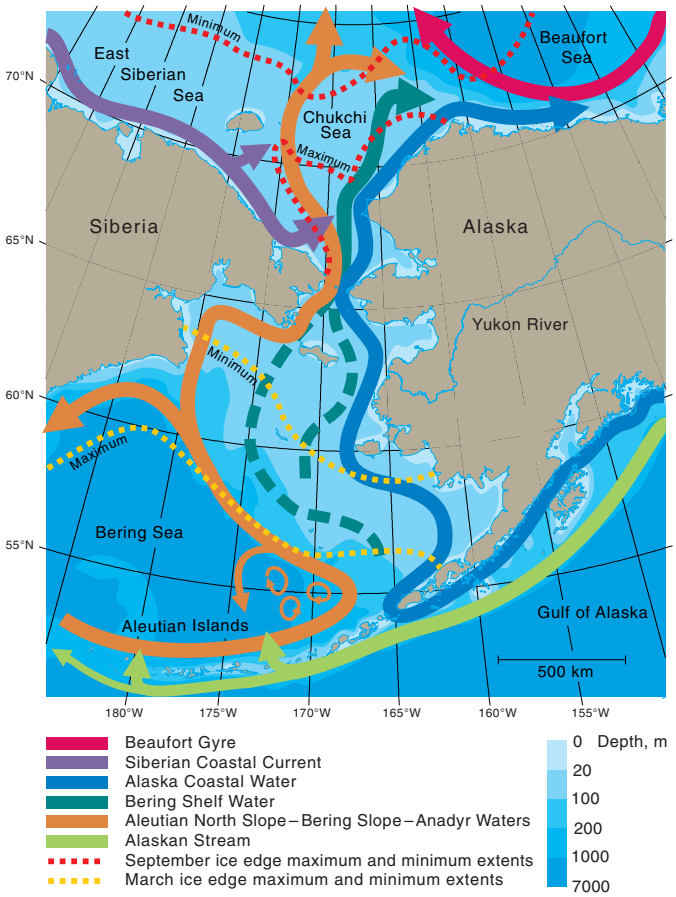

Figure 3·19. A schematic diagram of circulation in the Bering–Chukchi region of the Arctic. Flow over the Bering Sea shelf consists of waters from the Alaskan Stream, which feeds the Bering Slope Current, and fresher water from the Gulf of Alaska shelf which contributes to northward transport over the eastern Bering Shelf. In the Chukchi region, the Siberian Coastal Current transports fresh, cold water from the East Siberian Sea. Maximum (March) and minimum (September) ice coverage and their variations are shown by dashed lines (adapted from NOCD, 1986).

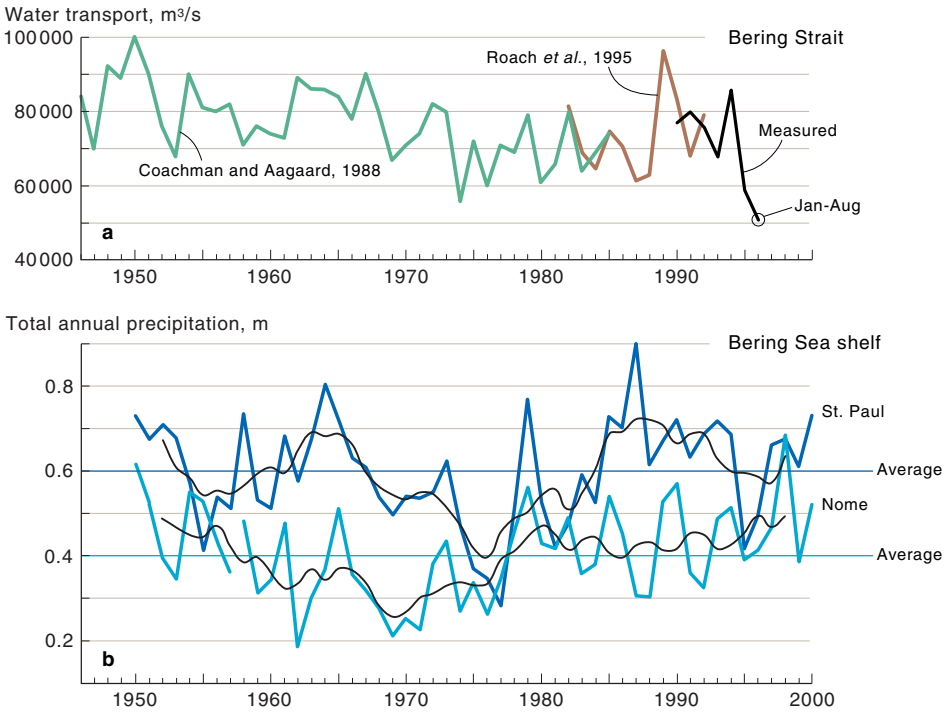

Figure 3·20. Time series of a) mean annual transport of water through Bering Strait from 1946 to 1996 (adapted from Roach *et al.*, 1995) and b) precipitation over the Bering Sea shelf based on annual precipitation measurements.

fresh Pacific inflow plays an important role in stratifying the upper 200 m of the Canada Basin (Carmack, 1986; Coachman and Aagaard, 1974) and can be detected as far away as Fram Strait (Jones and Anderson, 1986; Newton and Sotirin, 1997). The freshness of Pacific waters is supported by river runoff onto the Bering Sea shelf, relatively fresh inflow from the Gulf of Alaska (Royer, 1982), and greater precipitation than evaporation over the North Pacific Ocean (Warren, 1983).

Any alteration in the global thermohaline circulation (occurring at time scales of hundreds of years) will probably lead to change in the amount and composition of water passing through Bering Strait (see, for example, Wijffels *et al.*, 1992). Interannual and decadal scale variations in water transport, which may account for 40% of the variation in the long-term mean, are predominantly forced by the regional winds (Figure 3·20 a) whose strength and direction depends on the intensity and position of the Aleutian Low (Figure 3·2). Variation on the decadal scale (water transport was 15% lower during 1973 to 1996 than during 1946 to 1972) has also been inferred from wind records (Figure 3·20 a).

Upwelled Pacific waters support one of the world's most productive ecosystems in the northern Bering–southern Chukchi Seas (Springer *et al.*, 1996; Walsh *et al.*, 1989), including both oceanic fauna and shelf fauna transported within the surface water flowing northward over the Bering shelf (Walsh *et al.*, 1989). These shelves also serve as an important migratory pathway and critical habitat for a rich and diverse group of marine mammals, birds, and fish that move between polar, temperate, and tropical waters (Ainley and DeMaster, 1990; Tynan and DeMaster, 1997).

Pacific waters are substantially modified over the shelves through exchanges with the land, atmosphere, seabed, ice cover, and through biogeochemical transformations within the water column. These processes, which vary tremendously on seasonal and interannual time scales, affect the fate and distribution of contaminants deposited in the northeast Pacific and the Bering and Chukchi Seas following atmospheric transport across the North Pacific from Asia (Li *et al.*, 2002; Macdonald and Bewers, 1996; Macdonald *et al.*, 2002b; Wilkening *et al.*, 2000).

Salinity variations of ~1 in the inflowing Pacific water (Roach *et al.*, 1995) correspond to a range in injection depth into the Arctic Ocean halocline of 80 m or more, which is significant in determining whether, or how, contaminants from the Pacific Ocean might enter Arctic Ocean food webs. Salinity variation over the Bering shelf is controlled partly by sea-ice production and melting and partly by net precipitation, this latter process being, itself, an important pathway for some contaminants (e.g., Li *et al.*, 2002). Precipitation exhibits interannual variations that are as high as 50% of the long-term average, and also decadal or longer cycles with, for example, the 1960s to 1970s being relatively dry (Figure 3·20 b).

The ice edge in the Bering–Chukchi Seas migrates annually as much as 1700 km between the southern Bering shelf in winter (lowest dashed line on Figure 3·19) to the northern Chukchi shelf in summer (highest dashed line on Figure 3·19) with interannual variability of as much as 400 km (Niebauer, 1998; Walsh and Johnson, 1979). Variability in ice cover is governed by the strength and position of the Aleutian Low and East Siberian High (Figure 3·2) which influence storm tracks across the North Pacific (Niebauer, 1998; Overland and Pease, 1982). In the Chukchi Sea, the summer and autumn ice edge position can vary by as much as 200 km from its seasonally adjusted mean location (NOCD, 1986), with this variability associated with wind anomalies (Maslanik *et al.*, 1999). A significant decrease in ice cover over the Bering Sea appears to have coincided with a shift in the late 1970s from the 'cold' phase of the Pacific Decadal Oscillation (PDO) (Figure 3·16 b) to its 'warm' phase (Figure 3·21, and see also Macklin, 2001; Niebauer, 1998).

In the Bering Strait, late summer and autumn water temperatures can exceed 7°C, with substantial year-to-year variability. This variability, which affects ice melt on the Chukchi shelf and possibly the developmental rates

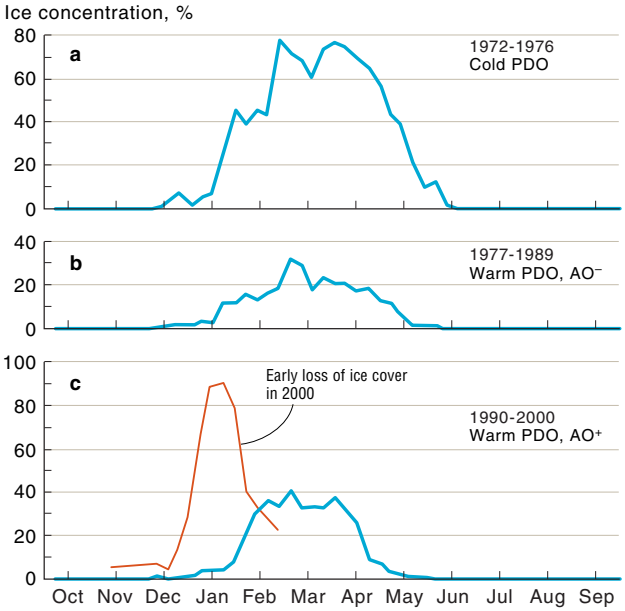

Figure 3·21. Ice concentration over the southeastern Bering Sea between 57°N and 58°N for a) a cold PDO phase (1972-76), b) a warm PDO and an AO⁻ phase (1977–89), and c) an intermediate regime with a warm PDO and an AO⁺ phase (1990-2000). Red line shows the early loss of ice cover in 2000 (adapted from Macklin, 2001).

of fish and other marine organisms, is related to change in large-scale advection and/or the summer radiation balance over the Bering Sea. Most of the ice in the Bering Sea grows and melts *in situ* such that brine rejection and melting strongly influence this shelf's water properties and stratification. During a spring and summer following heavy ice cover, the shelf water column is more strongly stratified and bottom temperatures are considerably lower (Azumaya and Ohtani, 1995), exerting a substantial influence on species composition and the distribution of marine fish, birds, and mammals (Wyllie-Echeverria and Ohtani, 1998; Wyllie-Echeverria and Wooster, 1998).

Ice cover also affects the carbon cycle. In spring, when nutrient concentrations are high, meltwater from sea ice stratifies the euphotic zone and initiates an ice edge bloom. Because zooplankton concentrations are low due to cold water temperatures, ungrazed phytoplankton settle to the seabed. In the absence of ice, water temperatures are warmer, phytoplankton are consumed by zooplankton, and less carbon is delivered to the benthos (Niebauer and Alexander, 1985).

Throughout spring and summer, waters of the central Bering shelf are strongly stratified owing both to the previous winter's ice history and to summer surface warming by solar radiation. Wind mixing is required to erode the stratification and replenish the euphotic zone with nutrients from depth. Springer (pers. comm., 2001.) shows that there is large interannual variability in wind speed, which provides the energy for mixing, and wind speeds over the Bering Sea seem to have diminished since the late 1970s by ~40%, coincident with the shift in the PDO from its cold phase to its warm phase.

The northward advection of warm water from the Bering Strait causes ice melt to occur earlier over the Chukchi shelf and freeze-up to be delayed, thereby prolonging the ice-free season relative to most other Arctic shelves (Martin and Drucker, 1997; Paquette and Bourke, 1981). Variability in flow through the Bering Strait (Figure 3·20 a), therefore, affects ice climate in the Chukchi Sea. Furthermore, variations in summer water properties and/or transport could lead to changes in the structure of shelf and slope food webs, insofar as the warm water provides suitable seasonal habitat for Pacific organisms advected into the Arctic (Melnikov *et al.*, 2002).

The volume and salinity of dense water formed over the Chukchi shelf each winter is affected by the extent of the seasonal retreat and advance of sea ice, which is variable and may change with warming. A thin ice cover in the autumn promotes early cooling of shelf waters, new ice growth, and the formation of multiple high-salinity water mass modes (Figure 3·22 a), whereas thick ice cover delays cooling, inhibits new ice growth, and leads to low-salinity water mass modes (Figure 3·22 b). These water masses then exchange differently with the interior ocean.

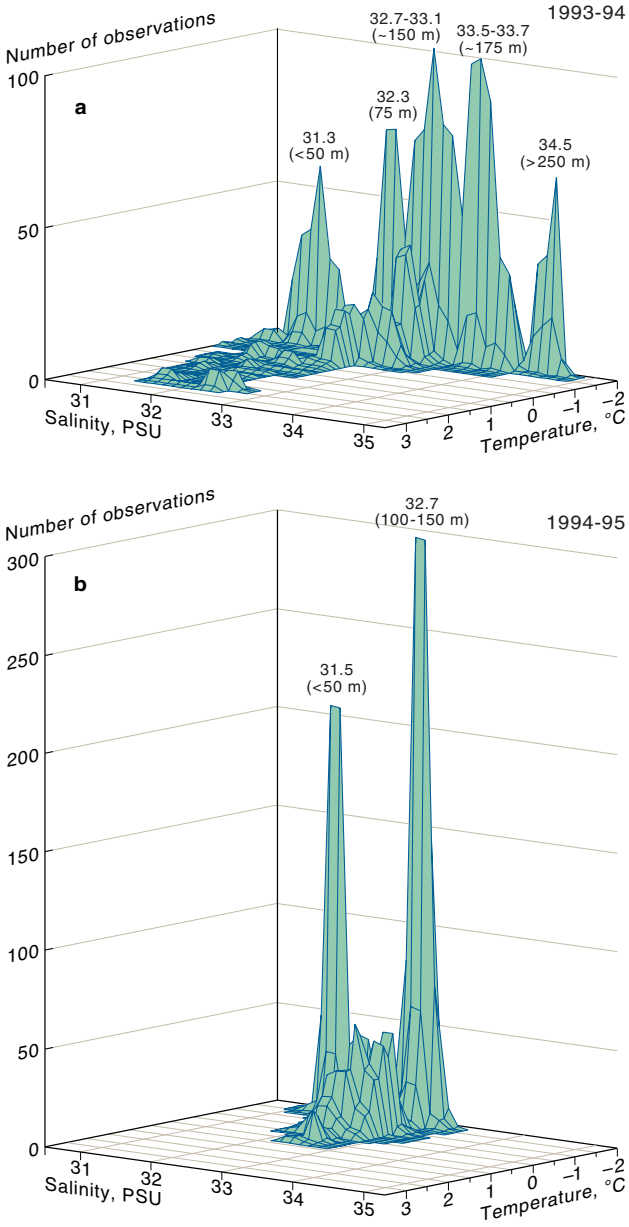

Figure 3·22. Water properties (T, S) on the northeastern Chukchi shelf in a) 1993-1994, with light autumn ice cover, large polynyas in winter, and multiple high-salinity water mass modes; and b) 1994-1999, with heavy autumn ice cover, small polynyas, and low-salinity water mass modes. The depths in parentheses refer to the depth to which each mode would sink along the continental slope if no mixing occurred.

The Siberian Coastal Current (SCC; Figure 3·19), flowing eastward along the Siberian coast for ~2000 km, also contributes low-salinity water to the Chukchi shelf (Coachman *et al.*, 1975; Weingartner *et al.*, 1999). From its probable origin in the western East Siberian Sea, the SCC draws water from as far as the Laptev Sea including ice melt and river discharges from the Lena, Indigirka, Kolyma and other Russian rivers along the way (Figure 1·1, Proshutinsky *et al.*, 1995). Zooplankton aggregate along the front between the SCC and the warmer, saltier water flowing through Bering Strait, providing important feeding opportunities for bowhead whales (*Balaena mysticetus*) in the western Chukchi Sea (Moore *et al.*, 1995) and potentially a critical pathway for contaminants to enter the food web at that point. Although transport in the SCC is relatively small (~3000 km^3/yr), its low-salinity waters enriched by runoff from Russian rivers could substantially dilute the inflow through Bering Strait and influence the distribution of Pacific waters in the Arctic Ocean.

The SCC exemplifies several ways in which changes in Arctic coastal currents can affect the transport and dispersal of contaminants (dissolved or sediment-bound). Firstly, coastal currents have large seasonal variability because 75 to 90% of the river discharge occurs within a three-month summer period. Change in the timing or amount of freshwater inflow will be expressed in the seasonal structure of the shelf circulation (Omstedt *et al.*, 1994). Secondly, coastal currents provide a vector to transport contaminants along a vast shoreline that can be dramatically altered by windfield change accompanying the AO (see Figure 3·14, section 3.5.2.1 and Guay *et al.*, 2001; Johnson and Polyakov, 2001; Weingartner *et al.*, 1999). Thirdly, river ice breakup typically occurs before the landfast ice melts with the result that little mixing initially occurs between the river water and the ambient shelf water and the inner shelf becomes strongly stratified (Ingram, 1981; Macdonald *et al.*, 1995). After the landfast ice melts, plume behaviour depends critically on the time-integrated effects of the wind velocity. Under 'upwelling' favourable winds, freshwater plumes can easily spread to interior basins carrying contaminants far beyond the shelf break (Macdonald *et al.*, 1999a). Under 'downwelling' favourable winds coastal currents are more likely to be formed (Melling, 1993; Weingartner *et al.*, 1999). Lastly, the dispersal and storage of freshwater over Arctic shelves in late summer set limits on the density of water that can be formed by sea-ice production the following winter (Macdonald, 2000; Melling, 1996; Weingartner *et al.*, 1999).

3.6.3. The Canadian Arctic Archipelago

The Canadian Arctic Archipelago provides one of the important outlets for Arctic Ocean surface water (Figure 1·1). Therefore, both changes in Arctic Ocean surface water contaminant burdens and changes in the source of water flowing out through the Archipelago have the potential to alter contaminant concentrations within the Archipelago's channels. There are few data with which to evaluate how seawater within the Archipelago channels responds to the AO. However, changes in distribution of surface water properties (Figures 3·13 and 3·14) and ice drift trajectories (Figure 3·9) in the Arctic Ocean itself, together with non-uniform spatial distribution of properties including river water and contaminants (e.g., see Carmack *et al.*, 1997; Guay and Falkner, 1997) should indicate the potential for upstream basin changes to be recorded as variable contaminant loadings in water flowing through the Archipelago. Furthermore, bowhead whale remains and driftwood on Archipelago shores suggest that ice-drift trajectories and ice cover have both varied greatly over time (Dyke *et al.*, 1996b, 1997; Dyke and Savelle, 2000, 2001) implying that the Canadian Arctic Archipelago is sensitive to rapid and dramatic change.

3.6.4. Hudson Bay

Hudson Bay is a large, shallow, semi-enclosed sea strongly influenced by seasonal runoff. The annual discharge (710 km^3/yr) is equivalent to a freshwater yield of about 65 cm (Prinsenberg, 1991). Presently, this sea exhibits a complete cryogenic cycle with summer (August-October) being ice free and winter fully ice covered. Climate models suggest that a doubling of CO_2 may lead to the virtual disappearance of ice from Hudson Bay thereby raising winter air temperatures and leading to the thawing of permafrost in adjacent land areas (Gough and Wolfe, 2001). These same models predict that the complete loss of ice will be preceded by years exhibiting earlier break-up and later freeze-up. According to Stirling and co-workers (1999), some of these projected changes may already be occurring (Figure 3·23), putting considerable stress on the western Hudson Bay polar bear (*Ursus maritimus*) population.

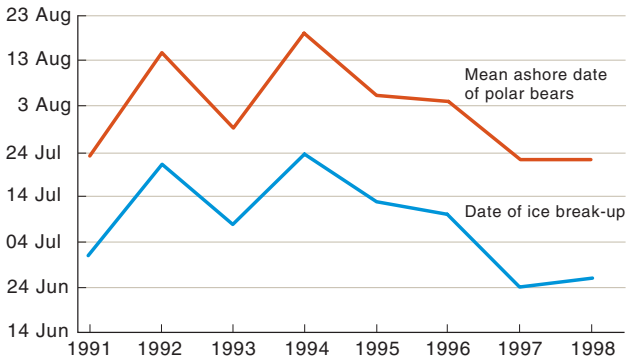

Figure 3·23. Temporal trends in the date of ice break up and the mean date at which polar bears return to shore in Hudson Bay. The break-up dates refer to that region in Hudson Bay where satellite-tagged female polar bears spent at least 90% of their time (modified from Stirling *et al.*, 1999).

The hydrological cycle of Hudson Bay has been strongly altered through immense damming projects in the drainage basin, leading to an increase in winter runoff to Hudson Bay of over 50% (Prinsenberg, 1991). Not only do such changes have an impact on stratification and hence nutrient cycling in this sea, but newly-flooded reservoirs are well known for their secondary effect of releasing mercury to downstream aquatic environments (Bodaly and Johnston, 1992).

Due to its southern location, Hudson Bay is clearly in the vanguard of Arctic change and is, therefore, a vital region to collect time series. According to Figure 3·3 a, Hudson Bay lies on a divide between warming and cooling. Regional temperature maps and other evidence

(Gilchrist and Robertson, 2000; Skinner *et al.*, 1998) confirm that between 1950 and 1990, the western side has warmed at about the same rate as the eastern side has cooled. In agreement with this observation, bears on the eastern side of Hudson Bay do not show the same pattern of weight loss as the bears on the western side (Stirling *et al.*, 1999), further emphasizing the importance of this region as a laboratory to study detailed consequences of change by contrast.

3.6.5. Baffin Bay, Davis Strait and the Labrador Sea

Baffin Bay, Davis Strait and the Labrador Sea occupy a unique position in that they may receive contaminants both from ice and water that exit the Arctic Ocean in the East Greenland Current and also from water and ice passing through the Canadian Arctic Archipelago. Change, therefore, can be produced by variation of contaminant composition within either of these sources or by altering their relative strength and the strength of direct exchange with the atmosphere. Furthermore, decadal-scale modulation probably differs for the various sources, with the AO perhaps influencing Archipelago through-flow or Fram Strait outflow, whereas the ice cover in Baffin Bay is more closely associated with the Southern Oscillation (Newell, 1996). In agreement with spatial temperature patterns (Figure 3·3 a), whereas ice season has been getting shorter within the Arctic Ocean and its marginal seas, Davis Strait and the Labrador Sea have recently exhibited an increase in the length of ice season (Parkinson, 1992).

Long-period cycles in the ice climate of this region (50 years or more) appear to have had dire consequences for both terrestrial and marine biological populations – including humans (Vibe, 1967). Like Hudson Bay, this appears to be an important region to study in the context of contaminants (Fisk *et al.*, 2001a), biogeographical variation (Johns *et al.*, 2001) and the impact of change on humans (Woollett *et al.*, 2000). Furthermore, surface water from Baffin Bay is exported to the south via Davis Strait to feed the Labrador Current (along with outflow from Hudson Bay and the Canadian Arctic Archipelago – Figure 1·1). Baffin Bay, therefore, provides a region of transition which can export change in ocean properties (freshwater, contaminants, biota) to the Northwest Atlantic.

3.7. Lake and river ice

Arctic lakes and rivers are likely to provide sensitive sentinels of climate change in their freeze, melt and hydrological cycles (Vörösmarty *et al.*, 2001). Whereas there appear to be no studies showing a relationship between freshwater ice cover and the AO, significant trends in these properties over the past 150 to nearly 300 years have been demonstrated (Magnuson *et al.*, 2000; Semiletov *et al.*, 2000). During the period between 1846 and 1995, there has been a mean delay of 5.8 days per century for freeze-up and a corresponding 6.5 days per century advance in break-up. This change in the freeze/melt cycle implies increasing temperatures of about 1.2°C per century.

Most Arctic lakes receive their contaminant burdens from the atmosphere, with the catchment area acting as a receptor through snow fall in winter, and a conveyor through runoff in spring. From a very limited set of studies, it appears that Arctic lakes presently retain only a small fraction of contaminant inputs because the main runoff pulse, which precedes lake turnover and peak primary production, simply traverses the lake surface under the ice (Macdonald *et al.*, 2000a). With lakes exhibiting more temperate characteristics, the coupling of runoff with lake mixing and primary production will change, probably allowing lakes to capture more of the inflowing contaminant burden. In particular, the potential for snow surfaces to enhance contaminant fugacity in lake settings is extremely large (Macdonald *et al.*, 2002c). However, quantitative measurements of contaminant–snow interactions are required because the significance of snow in contaminant cycling cannot be projected simply from hydrological measurements.

3.8. Permafrost

Permafrost underlies about 25% of the land in the Northern Hemisphere, including large areas of Canada, Russia, China and Alaska (Figure 3·24, Zhang *et al.*, 1999). Permafrost can also be found in sediments of the continental shelves (not shown). Especially vulnerable to change are regions of discontinuous permafrost which include large parts of northern Canada, Alaska and Russia. The IPCC (2002) suggests that permafrost area could be reduced by 12 to 22% by 2100 with perhaps as much as half of the present-day Canadian permafrost disappearing.

In regions of permafrost, the active layer of soil, typically limited to the top 1 m, supports almost all of the biological processes. The loss of permafrost, therefore, alters these biological processes, including affecting the kind of vegetation that can grow, and changes the way soil interacts with the hydrological cycle (Osterkamp *et al.*, 2000; Vörösmarty *et al.*, 2001) both of which have consequences for contaminant transport. In particular, thawing frozen ground releases sediment, nutrients, and

Figure 3·24. The distribution of permafrost in northern landmasses (source: IPA, 2001).

organic carbon which then enter ground water, rivers and lakes to impact upon biological cycles (see, for example, the studies done in the Mackenzie Basin; Cohen, 1997a). The observed thawing trends in Alaska and Russia, but not in northeastern Canada, appear to match the observed trends in SAT (see Figure 3·3 a and Rigor *et al.*, 2000). Accelerated permafrost degradation during the 1990s can probably be ascribed at least partly to the AO (Morison *et al.*, 2000) with, for example, the advection of warm air into the Russian Arctic during strong AO^+ conditions contributing to thawing in that region.

In addition to the changes in biogeochemical pathways that will accompany permafrost degradation, there will also be the widespread problem of re-mobilization of contaminants (see, for example, conference proceedings dedicated to the issue of contaminants in frozen ground; Anon., 2001a,b). Historical disposal of waste substances has occurred in the form of sewage lagoons, dump sites at DEW line sites (Distant Early Warning Line; a chain of defense radar stations, many now abandoned, along 66°N in Canada, also extending into Alaska and Greenland), solid waste dumps in small Arctic communities, mine tailings, and oil drilling sumps. A large component of the containment strategy for these sites is the presence of permafrost. With permafrost degradation, landfills can become washed directly into rivers or the ocean, or runoff can leach contaminants into local groundwater. In locations such as river deltas and coastal plains, low relief may provide a shortcut between such waste sites and drinking water.

3.9. Glacial ice

Most Arctic glaciers have experienced net loss in ice mass over the past few decades (Dowdeswell *et al.*, 1997). The Greenland ice mass appears presently (1994-1999) to be decreasing, predominantly at lower elevations, at a rate of about 51 km^3/yr (Krabill *et al.*, 2000). Data also point clearly to loss of ice mass for small glaciers in the Arctic during the interval between 1961 and 1993 (Arendt *et al.*, 2002; Dyurgerov and Meier, 1997; Serreze *et al.*, 2000). Since about 1960, glacial melt-back in the Canadian Arctic alone (Figure 3·25) is estimated at over 800 km^3 – around half of the melt-back estimated for the whole Arctic (Dyurgerov and Meier, 1997). In conformity with the strong AO^+ conditions of the early 1990s, the loss of glacial ice mass in the Canadian Arctic Archipelago was exceptionally strong in the early 1990s, amounting to 390 km^3 (Figure 3·25).

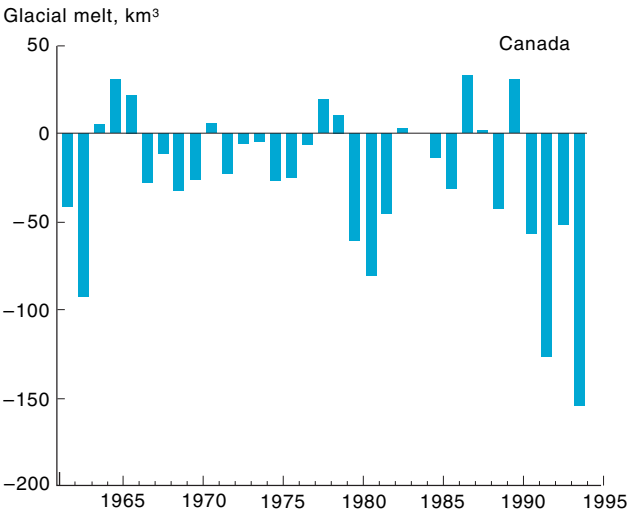

Figure 3·25. The loss of glacial ice mass, km^3/yr, in the Canadian Arctic between 1961 and 1993 based on data compiled by Serreze *et al.* (2000) and Dyurgerov and Meier (1997).

Glaciers may act as long-term reservoirs, sequestering and preserving airborne contaminants during peak emission years (1950-1970) later to release them during periods of melt-back (Blais *et al.*, 1998).